

AF EOAR 63-58

SR-4

December 1965

TECHNION RESEARCH & DEVELOPMENT

FOUNDATION, HAIFA, ISRAEL

630392



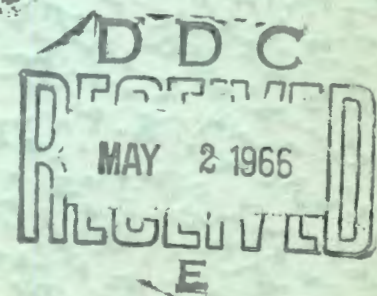
SCIENTIFIC REPORT No. 4

ON THE STABILITY OF ECCENTRICALLY STIFFENED
CYLINDRICAL SHELLS UNDER AXIAL COMPRESSION

Josef Singer, Menahem Baruch and Ovadia Harari

Technion - Israel Institute of Technology,
Department of Aeronautical Engineering.
Haifa, Israel.

TAE REPORT No. 44



Recd.

SCIENTIFIC REPORT No. 4

**ON THE STABILITY OF ECCENTRICALLY STIFFENED
CYLINDRICAL SHELLS UNDER AXIAL COMPRESSION**

Josef Singer, Menahem Baruch and Ovadia Harari

Technion - Israel Institute of Technology

Department of Aeronautical Engineering

Haifa, Israel.

TAE REPORT No. 44

S U M M A R Y

The eccentricity effect of stiffeners is studied for stiffened cylindrical shells under axial compression. Classical simple supports and classical clamped ends are considered. A detailed physical explanation of the causes of the eccentricity effect and its behavior is proposed and verified by computations for 350 typical shells.

As for buckling under hydrostatic pressure and torsion studied earlier, the behavior of the eccentricity effect in the case of axial compression also depends very strongly on the geometry of the shell, represented by the Batdorf parameter, while the geometry of the stiffeners only influences its magnitude. Inversion of eccentricity effect occurs at very low Z , but for practical dimensions outside stringers always stiffen the shell more than inside ones. The eccentricity effect has a pronounced maximum at practical values of Z , and the behavior of the eccentricity effect is very similar for clamped and simply supported shells. Rings, which are much less effective stiffeners than stringers under axial compression, are also considered. Results are compared with those of other investigators.

TABLE OF CONTENTS

	<i>Page</i>
SUMMARY	I
LIST OF FIGURES	III
LIST OF TABLES	IV
LIST OF SYMBOLS	V
SECTION 1. INTRODUCTION	1
SECTION 2. SIMPLY SUPPORTED SHELLS	2
SECTION 3. CLAMPED SHELLS	6
SECTION 4. PHYSICAL EXPLANATION	10
SECTION 5. NUMERICAL RESULTS AND DISCUSSION	16
SECTION 6. CONCLUSIONS	22
ACKNOWLEDGEMENT	22
REFERENCES	23

LIST OF FIGURES

- Fig. 1 - Notation
- Fig. 2 - The primary eccentricity effect
- Fig. 3 - The secondary eccentricity effect
- Fig. 4 - Influence of Poisson's ratio on eccentricity effect
- Fig. 5 - Variation of eccentricity effect with shell geometry and boundary conditions.
- Fig. 6 - Effect of end conditions on the structural efficiency of eccentrically stiffened shells.
- Fig. 7 - Effect of stiffener geometry on stiffening of shell
- Fig. 8 - Influence of (A_1/bh) on eccentricity effect
- Fig. 9 - Influence of magnitude of $|e_1/h|$ on eccentricity effect
- Fig. 10 - Influence of torsional rigidity of stringers on stiffening of shell
- Fig. 11 - Corrected structural efficiency of stringer stiffened cylindrical shell with simple supports
- Fig. 12 - Influence of stiffener cross-sectional area on structural efficiency of simply supported shell.

LIST OF TABLES**Table No.**

- 1 - Axial Load Parameter λ for Stringer Stiffened Cylinders - Effect of Shell Geometry for Clamped and Simply Supported Boundary Conditions.
- 2 - Axial Load Parameter λ for Stringer Stiffened Cylinders - Effect of Shell Geometry
- 3 - Axial Load Parameter λ for Stringer Stiffened Cylinders - Effect of Stringer Geometry
- 4 - Influence of Poisson's Ratio on Eccentricity Effect
- 5 - Eccentricity Effect for Cylindrical Shells with Heavy Stringers
- 6 - Ring Stiffened Cylinder under Axial Compression - Axisymmetric and Non-Axisymmetric Buckling
- 7 - Influence of Torsional Rigidity of Stringer (η_{t1}) on Buckling Load.
- 8 - Comparison of Theory with Card's Experimental Results.

S Y M B O L S

A_n, B_n, C_n	- coefficient of displacements
A_1	- cross-sectional area of stringer
A_2	- cross-sectional area of frame (ring)
a	- distance between frames (rings)
a_q, b_q	- defined by Eq. (20)
b	- distance between stringers
D	- $[Eh^3 / 12(1-\nu^2)]$
D_{0q}, D_{1q}, D_{2q}	- defined by Eqs. (21)
E, E_1, E_2	- moduli of elasticity of shell, stringers and frames, respectively
e_1, e_2	- distance between centroid of stiffener cross-section and middle surface shell, positive when inside (see Fig. 1)
$F(q)$	- defined by Eq. (22)
G_1, G_2	- shear moduli of stringers and frames, respectively
h	- thickness of shell
I_{11}, I_{22}	- moment of inertia of stiffener cross-section about its centroidal axis
I_{01}, I_{02}	- moment of inertia of stiffener cross-section about the middle surface of the shell
I_{t1}, I_{t2}	- torsion constant of stiffener cross-section
L	- length of shell between bulkheads
$M_x, M_\phi, M_{x\phi}$	- moment resultants acting on element

VI

\bar{M}_x	- geometrical bending stiffness of stringer-shell combination
m	- integer
$N_x, N_\phi, N_{x\phi}$	- membrane force resultants acting on element
n	- number of half longitudinal waves
$N_{x0}, N_{\phi0}, N_{x\phi0}$	- prebuckling membrane force resultants
p	- hydrostatic pressure
P	- axial load
\bar{P}	- buckling load of equivalently thickened shell computed with empirical buckling coefficients
P_{UNS}	- buckling load for unstiffened shell
$P_{UNS. EQ.}$	- buckling load of equivalently thickened shell
P_{cor}	- buckling load of monocoque cylinders corrected by empirical coefficients
q	- (n-1) or (n+1)
R	- radius of shell
t	- number of circumferential waves
u^*, v^*, w^*	- displacements [see Fig. 1]
u, v, w	- non-dimensional displacements ($=u^*/R$; v^*/R ; w^*/R respectively)
x^*, z^*, ϕ	- co-ordinates (see Fig. 1)
x, z	- non-dimensional co-ordinates ($=x^*/R$; z^*/R)
Z	- $(1-\nu^2)^{1/2} (L/R)^2 (R/h)$

VII

z_1	-	distance of the centroid of the stringer-shell combination from the middle surface (see Fig.2)	
β	-	$\pi R/L$	
$\gamma_{x\phi}$	-	$u_{,x} + v_{,\phi}$	} middle surface strains
ϵ_x	-	$u_{,x}$	
ϵ_ϕ	-	$v_{,\phi} - w$	
ζ_1	-	$(E_1 A_1 e_1 R/bD)$	
ζ_2	-	$(E_2 A_2 e_2 R/aD)$	
η_{01}	-	$(E_1 I_{01}/bD)$	
η_{02}	-	$(E_2 I_{02}/aD)$	
η_{t1}	-	$(G_1 I_{t1}/bD)$	
η_{t2}	-	$(G_2 I_{t2}/aD)$	
κ_x	-	$w_{,xx}$	} non dimensional changes of curvature and twist of the middle surface
κ_ϕ	-	$w_{,\phi\phi}$	
$\kappa_{x\phi}$	-	$w_{,x\phi}$	
λ	-	$PR/\pi D$ (when written with the superscript + or - it means axial load parameter for inside or outside stiffened shell)	
λ_{UNS}	-	λ for unstiffened shell,	
λ_p	-	$(R^3/D)p$	
μ_1	-	$(1-\nu^2)(E_1 A_1/Ebh)$	

VIII

- μ_2 - $(1-\nu^2)(E_2A_2/Eah)$
- ν - Poisson's ratio
- x_1 - $(1-\nu^2)(E_1A_1e_1/EbhR)$
- x_2 - $(1-\nu^2)(E_2A_2e_2/EahR)$

Subscripts following a comma indicate differentiation.

1. INTRODUCTION

In 1947 van der Neut [1] showed, for the case of buckling under axial compression, that the eccentricity of stiffeners with respect to the skin has great importance. Later some analyses of bending and buckling under external pressure, [2] - [4], took the effect of eccentricity into account, but the importance of placing the stiffeners on the inside or outside of the shell for external pressure loading was only recently emphasized [5]. The simple method of analysis of [5] has also been employed for the analyses of stiffened conical shells under hydrostatic pressure, [6] and [7].

Experimental evidence of the importance of the eccentricity of stiffeners was first given by tests carried out at the College of Aeronautics, Cranfield [8] and more recently by the spectacular results of tests at the NASA Langley Research Center [9] and of tests performed by the Lockheed Missiles and Space Company [10]. Further recent experimental evidence can be found in tests on Mylar cylinders carried out at the DFL in Germany [11].

Many investigators have recently studied the effect of eccentricity of stiffeners on the buckling of cylindrical shells, especially for the case of axial compression, [12] to [18] and [10], and a partial physical explanation of the effect in stringer stiffened shells has recently been given by Thielemann and Esslinger [19]. However, in view of the inversion of the eccentricity effect, first noted in stiffened conical shells under hydrostatic pressure [7] and later investigated in detail for cylindrical shells under external pressure and torsion in [20] and [21] and also found in the calculations of [15] and [17], a closer look at the effect in axially compressed shells is warranted.

In [20] a more complete physical explanation of the eccentricity effect for ring and stringer stiffened shells under external pressure was presented and the physical arguments were verified by extensive calculations, covering a wide range of shell and stiffener geometries. A similar approach is adopted here. A detailed physical explanation of the phenomena is given and then the numerical results are analysed in the light of the expected physical behavior. The eccentricity effect is again shown to be made up of two opposing contributions: the primary effect - the influence of the membrane stresses in the shell on the bending stiffness of the shell-stiffener combination; and the secondary effect - the influence of the bending strains on the membrane stresses in the shell. The influence of the variation in shell and stiffener

geometry on the eccentricity effect is then explained by the interplay of the two effects. Inversion of the eccentricity effect is therefore possible also in axially compressed shells, but here it occurs only for extremely short shells which have no practical application. Again, the behavior of the eccentricity effect depends very strongly on the geometry of the shell, while the geometry of the stiffeners only influences its magnitude. In the case of axial compression, the eccentricity effect has a pronounced maximum which occurs for values of the Batdorf parameter, $Z = (1 - \nu^2)^{1/2} (L^2/Rh)$, representing dimensions commonly used in aerospace practice. Since very large eccentricity effects can be obtained in axially compressed cylindrical shells of practical dimensions, the design implications of variation in shell and stiffener geometry is also studied.

The analysis is an extension of that presented in [5]. However, since here axisymmetric buckling may also be important, the axisymmetric case is added. The analysis of [5] is then extended to clamped cylindrical shells in order to study the effect of rotational restraint at the boundaries on the eccentricity effect. Classical clamped ends, as given for example in [22] are considered. In view of recent work on the effect of the "secondary" boundary conditions on the buckling load of unstiffened cylindrical shells (see for example [23] - [25]), consideration of only 2 of the 8 possible end conditions may seem incomplete. However, from a recent study of the effect of boundary conditions on the buckling of orthotropic cylindrical shells [26], it appears that the effect of the secondary boundary conditions may be less pronounced in stiffened shells than in unstiffened ones, whereas restraint of end rotations is more important in stiffened shells. The comparison between classical simple supports and clamped ends is therefore significant. A more complete investigation of the effect of the boundary conditions has also been initiated at the Technion to reevaluate the conclusions of this comparison.

2. SIMPLY SUPPORTED SHELLS

For simply supported shells the analysis for nonaxisymmetric buckling is identical to that of [5] and [20], except for different prebuckling stresses. Hence only the main assumptions of the analysis are repeated and then the final results for axial compression are presented. The main assumptions are:

- a) The stiffeners are "distributed" over the whole surface of the shell.

- b) The normal strains $\epsilon_x(z)$ and $\epsilon_\phi(z)$ vary linearly in the stiffener as well as in the sheet. The normal strains in the stiffener and in the sheet are equal at their point of contact.
- c) The stiffeners do not transmit shear. The shear membrane force $N_{x\phi}$ is carried entirely by the sheet.
- d) The torsional rigidity of the stiffener cross section is added to that of the sheet (the actual increase in torsional rigidity is larger than that assumed).

The middle surface of the shell is chosen as reference line and the expressions for forces and moments in terms of displacements are :

$$\begin{aligned} N_x &= [Eh/(1-\nu^2)] [u_{,x}(1+\mu_1) + \nu(v_{,\phi} - w) - \chi_1 w_{,xx}] \\ N_\phi &= [Eh/(1-\nu^2)] [(v_{,\phi} - w)(1+\mu_2) + \nu u_{,x} - \chi_2 w_{,\phi\phi}] \\ N_{x\phi} = N_{\phi x} &= [Eh/2(1+\nu)] (u_{,\phi} + v_{,x}) \end{aligned} \quad (1)$$

$$\begin{aligned} M_x &= -(D/R) [w_{,xx}(1+\eta_{01}) + \nu w_{,\phi\phi} - \zeta_1 u_{,x}] \\ M_\phi &= -(D/R) [w_{,\phi\phi}(1+\eta_{02}) + \nu w_{,xx} - \zeta_2 (v_{,\phi} - w)] \\ M_{x\phi} &= +(D/R) [(1-\nu) + \eta_{t1}] w_{,x\phi} \\ M_{\phi x} &= -(D/R) [(1-\nu) + \eta_{t2}] w_{,x\phi} \end{aligned} \quad (2)$$

where μ_1 , μ_2 , η_{01} , η_{02} , η_{t1} and η_{t2} are the changes in stiffnesses due to stringers and frames and χ_1, χ_2 , ζ_1 and ζ_2 are the changes in stiffnesses caused by the eccentricities of the stringers and rings, as in [5]. Since the analysis is concerned with instability, u , v and w are the additional displacements during buckling, and as in [5] they are non-dimensional, the physical displacements having been divided by the radius of the shell.

The classical simple support boundary conditions

$$\begin{aligned}
 w &= 0 \\
 M_x &= 0 \\
 N_x &= 0 \\
 v &= 0
 \end{aligned}
 \tag{3}$$

are assumed and

$$\begin{aligned}
 u &= A_n \sin t\phi \cos n\beta x \\
 v &= B_n \cos t\phi \sin n\beta x \\
 w &= C_n \sin t\phi \sin n\beta x
 \end{aligned}
 \tag{4}$$

are the displacements which solve the Donnell type stability equations for general instability, Eq. (12) of [5], in the presence of these boundary conditions.

Assuming that the prebuckling stresses are represented satisfactorily by the membrane stresses

$$\begin{aligned}
 N_{x0} &= -(P/2\pi R) \\
 N_{\phi 0} &= 0 \\
 N_{x\phi 0} &= 0
 \end{aligned}
 \tag{5}$$

the third stability equation, Eq. (18) of [5], becomes for the case of axial compression

$$\begin{aligned}
 &\zeta_1(-n^3\beta^3 a_n) + \zeta_2(-2t^2 - b_n t^3) + \\
 &+ (1 + \eta_{01})n^4\beta^4 + (2 + \eta_{t1} + \eta_{t2})n^2\beta^2 t^2 + (1 + \eta_{02})t^4 + \\
 &+ 12(R/h)^2 [(1 + \mu_2)(1 + b_n t) + \nu n\beta a_n] - \lambda(n^2\beta^2/2) = 0
 \end{aligned}
 \tag{6}$$

where λ is a non-dimensional axial load parameter defined by:

$$\lambda = (PR/\pi D) = [12(1 - \nu^2)PR/\pi Eh^3]
 \tag{7}$$

and a_n and b_n are given by Eqs. (16) of [5].

The integer values of t and n (the circumferential waves and axial half-waves, respectively) which make λ a minimum have to be chosen to yield the critical axial load.

In cylindrical shells subjected to axial compression, axisymmetric buckling may occur under certain conditions. The axisymmetric mode can be obtained from the non-axisymmetric analysis by letting $t=0$. However, for completeness, the axisymmetric case is briefly rederived here with axisymmetry assumed from the beginning.

For axisymmetry the displacements are

$$\begin{aligned} u &= A_n \cos n\beta x &) \\ v &= 0 &) \\ w &= C_n \sin n\beta x &) \end{aligned} \quad (8)$$

and the stability equations become

$$\begin{aligned} N_{x,x} &= 0 &) \\ \text{and} & &) \\ M_{x,xx} + RN_\phi + N_{x0}Rw_{,xx} &= 0 &) \end{aligned} \quad (9)$$

The force and moment expressions are

$$\begin{aligned} N_x &= [Eh/(1-\nu^2)] [(1+\mu_1)u_{,x} - \nu w - \chi_1 w_{,xx}] \\ N_\phi &= [Eh/(1-\nu^2)] [-(1+\mu_2)w + \nu u_{,x}] \\ M_x &= (-D/R) [(1+\eta_{01})w_{,xx} - \zeta_1 u_{,x}] \\ M_\phi &= (-D/R) [\nu w_{,xx} + \zeta_2 w] \end{aligned} \quad (10)$$

Substitution of Eqs.(8) and (10) into Eqs.(9) yields

$$A_n = [1/n\beta(1+\mu_1)] [\chi_1(n\beta)^2 - \nu] C_n = a_n C_n \quad (11)$$

and

$$-\zeta_1 n^3 \beta^3 a_n + (1 + \eta_{01}) n^4 \beta^4 + 12(R/h)^2 [1 + \mu_2 + \nu n \beta a_n] = \lambda (n^2 \beta^2 / 2) \quad (12)$$

where λ is again defined by Eq. (7).

Hence, after substitution for a_n from Eq. (11), Eq. (12) becomes

$$\lambda/2 = (1 + \eta_{01}) n^2 \beta^2 + [12(R/h)^2 / n^2 \beta^2] \{1 + \mu_2 - [(\nu - \chi_1 n^2 \beta^2)^2 / (1 + \mu_1)]\} \quad (13)$$

The integer value of n which makes λ a minimum has to be used in calculations. When the shell is stiffened by rings only, Eq. (13) simplifies to

$$\lambda = 2 \{ n^2 \beta^2 + [12(R/h)^2 (1 + \mu_2 - \nu^2) / n^2 \beta^2] \} \quad (14)$$

and if one assumes that there are many waves in the axial direction and that n can be treated as a continuous variable, the critical value of λ becomes

$$\lambda_{crit} = 8\sqrt{3}(R/h)\sqrt{1 + \mu_2 - \nu^2} = 8\sqrt{3}(R/h)\sqrt{(1 - \nu^2) [1 + (A_2/ah)]} \quad (15)$$

3. CLAMPED SHELLS

The analysis of [5] is now extended to clamped cylindrical shells and is presented for axial compression and hydrostatic pressure. The same assumptions are made as for the simply supported shells, except that the classical clamped boundary conditions

$$\begin{array}{rcl} w & = & 0 \quad) \\ & &) \\ w_{,x} & = & 0 \quad) \\ & &) \\ u & = & 0 \quad) \\ & &) \\ N_{x\phi} & = & 0 \quad) \end{array} \quad \dots \quad (16)$$

are considered instead of Eqs. (3). Displacements similar to those proposed by Batdorf [22] for unstiffened clamped cylindrical shells are assumed here

$$\begin{aligned}
 u &= \sum_{n=1}^{\infty} (1/2) [A_{1n} \sin(n-1)\beta x - A_{2n} \sin(n+1)\beta x] \sin t \phi \\
 v &= \sum_{n=1}^{\infty} (1/2) [B_{1n} \cos(n-1)\beta x - B_{2n} \cos(n+1)\beta x] \cos t \phi \\
 w &= \sum_{n=1}^{\infty} C_n (1/2) [\cos(n-1)\beta x - \cos(n+1)\beta x] \sin t \phi
 \end{aligned} \tag{17}$$

When the shell is subjected to both axial compression and hydrostatic pressure the prebuckling stresses are taken as the sum of the membrane stresses, Eqs. (5) of this report and Eqs. (13) of [5]. The Donnell type stability equations in terms of displacements, Eqs. (12) of [5], are then

$$\begin{aligned}
 & [Eh/(1-\nu^2)] \{ (1+\mu_1) u_{,xx} + [(1-\nu)/2] u_{,\phi\phi} + [(1+\nu)/2] v_{,x\phi} - \chi_1 w_{,xxx} - \nu w_{,x} \} = 0 \\
 & [Eh/1-\nu^2] \{ [(1+\nu)/2] u_{,x\phi} + (1+\mu_2) v_{,\phi\phi} + [(1-\nu)/2] v_{,xx} - (1+\mu_2) w_{,\phi} - \chi_2 w_{,\phi\phi\phi} \} = 0 \\
 & (-D/R) \{ \zeta_1 (-u_{,xxx}) + \zeta_2 (2w_{,\phi\phi} - v_{,\phi\phi\phi}) + (1+\eta_{01}) w_{,xxxx} + (2+\eta_{t1} + \eta_{t2}) w_{,xx\phi\phi} + \\
 & \quad + (1+\eta_{02}) w_{,\phi\phi\phi\phi} + 12(R/h)^2 [(1+\mu_2)(w - v_{,\phi}) - \nu u_{,x}] + \lambda (w_{,xx}/2) + \\
 & \quad + \lambda_p [(w_{,xx}/2) + w_{,\phi\phi}] \} = 0 \quad \dots \tag{18}
 \end{aligned}$$

The first two of the stability equations, Eqs. (18), are solved by the assumed displacements, Eqs. (17), in the same manner as in [5]. The displacements can then be written as

$$\begin{aligned}
 u &= \sum_{n=1}^{\infty} C_n (1/2) \{ -a_{n-1} \sin[(n-1)\beta x] + a_{n+1} \sin[(n+1)\beta x] \} \sin t \phi \\
 v &= \sum_{n=1}^{\infty} C_n (1/2) \{ b_{n-1} \cos[(n-1)\beta x] - b_{n+1} \cos[(n+1)\beta x] \} \cos t \phi \\
 w &= \sum_{n=1}^{\infty} C_n (1/2) \{ \cos[(n-1)\beta x] - \cos[(n+1)\beta x] \} \sin t \phi \quad \dots \tag{19}
 \end{aligned}$$

where

$$\begin{aligned} a_q &= D_{1q}/D_{0q} \\ b_q &= D_{2q}/D_{0q} \end{aligned} \quad \dots (20)$$

and q represents $(n-1)$ and $(n+1)$ respectively

$$\begin{aligned} D_{0q} &= [(1-\nu)/2] \{ (1+\mu_2)t^4 + [(1+\mu_1)(1+\mu_2) - \nu] q^2 \beta^2 t^2 + \\ &\quad + (1+\mu_1)[(1-\nu)/2] q^4 \beta^4 \} \\ D_{1q} &= -[(1+\nu)/2] \chi_2 q \beta t^4 + (1+\mu_2) \chi_1 q^3 \beta^3 + [(1-\nu)/2] q \beta t^2 + \\ &\quad + \chi_1 [(1-\nu)/2] q^5 \beta^5 - \nu [(1-\nu)/2] q^3 \beta^3 \\ D_{2q} &= [(1-\nu)/2] \chi_2 t^5 + (1+\mu_1) \chi_2 q^2 \beta^2 - [(1-\nu)/2] (1+\mu_2) t^3 \\ &\quad + \left\{ [(1+\nu)/2] \nu - (1+\mu_1)(1+\mu_2) \right\} q^2 \beta^2 - [(1+\nu)/2] \chi_1 q^4 \beta^4 \} t \end{aligned} \quad \dots (21)$$

Note that D_{0q} , D_{1q} , and D_{2q} when $q = n$ are identical to D_{0n} , D_{1n} and D_{2n} given by Eqs. (17) of [5].

Here, however, the third of the stability equations, Eqs. (18), cannot be solved in closed form and hence it is solved by the Galerkin method. If one defines

$$\begin{aligned} F(q) &= \zeta_1 (-q^3 \beta^3 a_q) + \zeta_2 (-2t^2 - b_q t^3) + \\ &\quad + (1+\eta_{01}) q^4 t^4 + (2+\eta_{11} + \eta_{12}) q^2 \beta^2 t^2 + (1+\eta_{02}) t^4 + \\ &\quad + 12(R/h)^2 [(1+\mu_2)(1+b_q t) + \nu q \beta a_q] - \\ &\quad - \lambda (q^2 \beta^2 / 2) - \lambda_p [(q^2 \beta^2 / 2) + t^2] \end{aligned} \quad \dots (22)$$

the Galerkin integrals, for an N term solution, can be written as

$$\int_0^{2\pi} \sin^2 t \phi \left\{ \sum_{n=1}^N C_n \int_0^{L/R} F(n-1) \{ \cos[(n-1)\beta x] \cos[(m-1)\beta x] - \cos[(n-1)\beta x] \cos[(m+1)\beta x] \} - \right. \\ \left. - F(n+1) \{ \cos[(n+1)\beta x] \cos[(m-1)\beta x] - \cos[(n+1)\beta x] \cos[(m+1)\beta x] \} \right\} dx \Bigg\} d\phi$$

and $m = 1, 2, \dots, N$... (23)

Eqs. (23) yield a set of N algebraic equations

$$\sum_{n=1}^N C_n \{ F(n-1) [\bar{\delta}_{(n-1)(m-1)} - \bar{\delta}_{(n-1)(m+1)}] - F(n+1) [\bar{\delta}_{(n+1)(m-1)} - \bar{\delta}_{(n+1)(m+1)}] \} = 0$$

$$m = 1, 2, \dots, N \quad \dots \quad (24)$$

where

$$\bar{\delta}_{ij} = \delta_{ij} + \delta_{0j} \quad \dots \quad (25)$$

and δ_{ij} is the Kronecker delta defined by

$$\delta_{ij} = 0 \text{ when } i \neq j$$

$$\delta_{ij} = 1 \text{ when } i = j \quad \dots \quad (26)$$

The determinant of the coefficients of C_n in Eqs. (24), the stability determinant, can be resolved into two subdeterminants, one of the even components and one of the odd components representing symmetric and antisymmetric buckling modes. The symmetric buckling pattern is hence represented by

$$n = 1, 3, 5, \dots$$

$$m = 1, 3, 5, \dots$$

or the determinant

$$\begin{vmatrix}
 2F(0) + F(2) & -F(2) & 0 & 0 & \dots \\
 -F(2) & F(2) + F(4) & -F(4) & 0 & \dots \\
 0 & -F(4) & F(4) + F(6) & -F(6) & \dots \\
 0 & 0 & -F(6) & F(6) + F(8) & \dots \\
 \cdot & \cdot & \cdot & \cdot & \cdot \\
 \cdot & \cdot & \cdot & \cdot & \cdot \\
 \cdot & \cdot & \cdot & \cdot & \cdot
 \end{vmatrix} = 0 \tag{27}$$

and the antisymmetric buckling pattern by

$$n = 2, 4, 6, \dots$$

$$m = 2, 4, 6, \dots$$

or the determinant

$$\begin{vmatrix}
 F(1) + F(3) & -F(3) & 0 & 0 & \dots \\
 -F(3) & F(3) + F(5) & -F(5) & 0 & \dots \\
 0 & -F(5) & F(5) + F(7) & -F(7) & \dots \\
 0 & 0 & -F(7) & F(7) + F(9) & \dots \\
 \cdot & \cdot & \cdot & \cdot & \cdot \\
 \cdot & \cdot & \cdot & \cdot & \cdot \\
 \cdot & \cdot & \cdot & \cdot & \cdot
 \end{vmatrix} = 0 \tag{28}$$

The critical load has to be computed for both buckling patterns. However, the numerical work indicates that the antisymmetric mode usually yields higher buckling loads except for very long and thin shells. Hence Eq. (28) has to be considered only for long and thin shells.

4. PHYSICAL EXPLANATION

A physical explanation of the effect of eccentricity of rings on the instability of stiffened cylindrical

shells under hydrostatic pressure is given in [20]. There, the explanation is given for rings because rings are most effective in stiffening against hydrostatic pressure. For axial compression stringers are much more effective than rings and therefore the effect of the eccentricity of stringers will be considered here in detail.

The explanation follows the lines of that given in [20], but there are important differences between the behavior of stringer-stiffened shells under axial compression and that of ring-stiffened shells under hydrostatic pressure.

The total geometrical bending stiffness of the combined stringer-shell cross-section is not affected by the position of the stringers and is equal for outside and inside stringers. (Actually, the moment of inertia of the combined stringer-shell cross-section is larger for outside stringers but for closely spaced stringers this difference is small and can be neglected. When the closely spaced stringers are "distributed" there is no difference at all.) As a result of the initial curvature of the shell, additional membrane forces appear in it during buckling. If one considers the circumferential membrane forces, this is immediately apparent, since for outward buckles the shell has to lengthen and tensile forces arise, while for inward buckles the shell has to shorten and compressive forces arise.

A relation between the axial and circumferential membrane forces is obtained by differentiation of the first two stability equations (Eqs.(11) of [5] or Eqs.(4) of [20]) with respect to x and ϕ , which yields

$$N_{x,xx} = N_{\phi,\phi\phi} \quad (29)$$

By substitution of the assumed displacements for simple supports, Eqs. (4), into Eq. (29) this relation between the membrane forces becomes

$$n^2 \beta^2 N_x = t^2 N_\phi \quad (30)$$

As mentioned, N_ϕ is compressive in a positive (inward) wave and tensile in a negative wave. From Eq. (29) it is seen that N_x follows N_ϕ at every point of the shell.

It should be noted that Eq. (30) applies to the classical simple support boundary conditions Eqs. (3). For the classical clamped boundary conditions, Eqs. (16), a similar relation between N_x and N_ϕ can be obtained when $n = 1$, since substitution of Eqs.(19) into Eq.(29), with $n = 1$, yields

$$(n+1)^2 \beta^2 N_x = 4\beta^2 N_x = t^2 N_\phi \quad (31)$$

For $n \neq 1$ the relation cannot be expressed in such a simple manner, though it is similar in character. However, heavily stiffened cylindrical shells of practical dimensions tend to buckle with $n = 1$, unless they are very long. For long shells, the buckling pattern repeats itself, and though n increases, β decreases simultaneously, with the result that $n\beta$, which is really the important quantity in Eqs. (30) and (31), remains nearly constant. Hence the conclusions drawn from Eq. (30) apply approximately also to classical clamped ends, and may be expected to apply approximately also to the other boundary conditions not considered here.

In Figs. 2a to 2d, \bar{M}_x represents the geometrical bending stiffness of the cross-section of the stringer-shell combination. \bar{M}_x is the moment necessary to produce a certain change in curvature and is equal for inside and outside stringers. However, due to the longitudinal membrane force acting in the shell, the actual total bending stiffness of the cross-section is changed. For a stringer-shell combination with inside stringers the actual total bending stiffness is (see Figs. 2a and 2c)

$$M_x^{in} = \bar{M}_x - \bar{z}_1 N_x^{in} \quad (32)$$

where M_x^{in} is the actual moment necessary to produce the same change of curvature that \bar{M}_x would produce without the membrane force N_x^{in} .

In the same manner, the actual bending stiffness for the cross-section with outside stringers is (see Figs. 2b and 2d)

$$M_x^{out} = \bar{M}_x + \bar{z}_1 N_x^{out} \quad (33)$$

where again M_x^{out} is the actual moment necessary to produce the same change of curvature which \bar{M}_x would produce without the membrane force N_x^{out} .

From Eqs. (32) and (33) it can be seen that the actual bending stiffness for outside stiffening is larger than that for inside stiffening. This is the primary eccentricity effect. There is, however, another opposing secondary effect that influences the behavior of eccentrically stringer-stiffened shells under axial compression, though its influence is less noticeable here than for ring-stiffened shells under hydrostatic pressure.

Consider a shell with inside stringers. In a positive wave, the moment M_x produces in the shell an additional compressive strain in the longitudinal direction. Due to Poisson's effect (ν), a circumferential strain appears in the sheet, giving rise to an additional compressive membrane force, ΔN_ϕ , in the circumferential direction, which resists this strain. This additional compressive membrane force has a radial component which resists radial deformation (Fig. 3a). On the other hand, for outside stringers the additional force ΔN_ϕ is tensile and therefore assists deformation (Fig. 3b). In a negative wave (Figs.

3c and 3d) the same argument applies and the additional membrane force ΔN_ϕ , resists the deformation for inside stringers, whereas it assists it for outside stringers.

The effect of eccentricity of stringers can therefore be summarized as follows :

1. Primary effect – outside stringers increase the actual bending stiffness in the longitudinal direction more than inside stringers.
2. Secondary effect – inside stringers increase the actual extensional stiffness in the circumferential direction more than outside stringers.

Now, for short cylinders the main resistance to buckling is in the longitudinal direction. M_x is the main component of the resistance of the shell. N_x is very small and therefore the difference in the actual bending stiffness for inside and outside stringers is also small. Since M_x is large and the secondary effect is important for very short cylinders, inside stringers may yield larger critical axial loads than outside stringers, as is indeed found in the computations. It should be remembered that the secondary effect depends entirely on Poisson's ratio ν . Variation of ν will therefore noticeably influence the secondary effect. With $\nu = 0.5$ the secondary effect is enhanced while with $\nu = 0$ it vanishes, as is later verified in the numerical work.

For medium length cylinders M_x is still important, but N_x increases and therefore the difference between the actual longitudinal bending stiffnesses for outside and inside stringers also increases. Hence the critical axial load is much larger with stringers on the outside than on the inside of the shell.

For long cylinders, the difference between the actual longitudinal bending stiffnesses for outside and inside stringers continues to increase. The contribution of the membrane force to the actual total bending stiffness, $Z_1 N_x$, becomes larger than M_x and for inside stringers the actual bending stiffness, M_x^{in} , may even change sign and become negative. This has been verified for a typical long shell.

However, the total difference between the critical axial load for outside and inside stringers decreases as the length of the shell increases, or more precisely, as Z increases. This is caused by the diminishing relative importance of M_x and N_x in resisting buckling for long shells, in which M_ϕ is the main element of the buckling strength of the shell. Since M_ϕ is not affected by the eccentricity of the stringers, the total eccentricity effect declines in long shells.

Rings are much less effective than stringers in stiffening of cylindrical shells subjected to axial compression. The behavior of ring stiffened shells under axial compression is, however, of interest, since shells primarily designed to withstand lateral pressure (which will be predominantly ring stiffened) may also be subjected to axial loads under certain conditions.

The eccentricity effect of rings in an axially compressed cylindrical shell is basically the same as that considered above for stringers and given in detail for ring stiffened shells subjected to hydrostatic pressure in [20]. The same primary and opposing secondary effects could be discerned and ranges should occur where the primary effect dominates and outside rings yield higher buckling loads than inside rings, and where the secondary effect dominates and inside rings are better. However, under axial compression ring stiffened shells buckle with many longitudinal waves, unless the shell is very short, and hence subdivide into many short "bays". As a result, the axially compressed ring-stiffened shell is always in the "short shell" range where outside rings should yield higher buckling loads than inside ones. The computations verify this argument.

The discussion up to this point has only considered non-axisymmetric buckling patterns, and the possibility of axisymmetric buckling has now to be considered. Since in the axisymmetric buckling pattern no bending occurs in the circumferential direction, the eccentricity of rings cannot affect the critical load when the shell buckles in this mode. This is verified by the axisymmetric analysis, see Eq. (13), where no terms containing the eccentricity of rings appear. Only the added area of the rings stiffens the shell against circumferential extension and compression, but this stiffening is the same for outside and inside rings.

One should now remember that for isotropic cylindrical shells under axial compression the classical buckling load is the same for axisymmetric and non-axisymmetric buckling, provided $n\beta$ and t (the longitudinal wave parameter and the number of circumferential waves) are large enough to be considered continuous, or is approximately the same otherwise, see for example [27]. From an energy point of view this means that the same amount of strain energy is absorbed by a shell buckling in an axisymmetric pattern (sometimes called ring-shape pattern) and by one buckling in a non-axisymmetric pattern (sometimes called chess-board pattern).

For ring-stiffened shells this is no longer so. Consider first centrally placed rings ($e_2 = 0$). As

was already found by Thielemann for orthotropic shells [28], the classical linear theory buckling loads, characterized by chess-board (asymmetric) and ring-shape (axisymmetric) buckling, no longer coincide in general. For a ring-stiffened cylindrical shell the chess-board pattern usually yields a slightly lower buckling load than the ring-shape pattern. This may be explained by energy considerations. The cross-sectional area added to the shell by the rings stiffens it considerably against circumferential extension or compression. Axisymmetric buckling, in which most of the strain energy absorbed is the extensional strain energy due to the circumferential extension and compression of the shell, would therefore require appreciably more energy input. On the other hand, in non-axisymmetric buckling only a smaller fraction of the strain energy is absorbed in extensional deformation and the remainder is due to bending in the longitudinal and circumferential directions. For a hypothetical shell, in which the rings add only cross-sectional area but no increase in moment of inertia in the circumferential direction, the chess-board pattern will obviously yield a lower buckling load than the ring-shape pattern. For, in comparison to an unstiffened shell, the increase in area in the stiffened shell due to the rings affects a smaller portion of the total strain energy in non-axisymmetric buckling than in the axisymmetric pattern. As the moment of inertia of the rings is increased, for constant cross sectional area, the energy absorbed by circumferential bending increases and the buckling load of the chess-board pattern rises and approaches that for the ring-shape pattern. For fairly large I_{22} , non-axisymmetric buckling would require more energy input than symmetric buckling, and hence above a certain magnitude of I_{22} the shell will always buckle in an axisymmetric pattern. This is verified by computations for a typical shell (see Table 6).

When the rings are eccentrically positioned, outside rings should yield higher buckling loads than inside ones in non-axisymmetric buckling, since axially compressed ring-stiffened shells are always in the "short" shell range. With inside rings, non-axisymmetric buckling will occur and the positive eccentricity will lower the buckling below that for centrally placed rings. With outside rings, however, the increase in buckling load that would result from the negative eccentricity if the shell were to buckle in a chess-board pattern, is not realized, since the shell now buckles in the ring-shape pattern which is unaffected by eccentricity and yields a lower buckling load. In shells with very small negative eccentricity and small I_{22} , chess-board patterns are still possible, but for practical dimensions the axisymmetric buckling mode always predominates in this case. Computations for typical shells verify the arguments

presented.

For design purposes, the small differences between axisymmetric and non-axisymmetric buckling for centrally placed or outside rings, discussed above, may be neglected. One can therefore conclude roughly that with inside rings a chess-board pattern occurs and the buckling load is reduced by the eccentricity of the rings, whereas with outside rings the axisymmetric pattern dominates and the magnitude of the eccentricity does not affect the buckling load.

5. NUMERICAL RESULTS AND DISCUSSION

The critical axial loads have been computed for 350 ring and stringer stiffened shells covering a wide range of shell and stiffener geometries.

The computations were carried out on the Elliot 803 and 503 computers of the Technion computation center. The shell and stiffener geometries and the resulting critical load parameters are given in Tables 1 to 8.

In order to study the behavior of the secondary effect, the variation of the total eccentricity effect, (P^{out}/P^{in}) , with Z is plotted for different values of Poisson's ratio in Fig. 4. The extreme values of ν considered, $\nu = 0$ and $\nu = 0.5$ are unrealistic, but bring out very clearly the dependence of the secondary effect on ν . With $\nu = 0$ the secondary effect disappears, while with $\nu = 0.5$ it is enhanced. For very small values of Z , the curves for $\nu = 0.5$ fall below $(P^{out}/P^{in}) = 1$. Hence an inversion of the eccentricity effect is demonstrated. In the range of Z below the inversion point, inside stringers yield higher buckling loads than outside ones. There the primary effect is overshadowed by the secondary effect as the result of the growing importance of M_x relative to N_x . For $\nu = 0$ there is no inversion and the curve tends asymptotically (from the positive side) to $(P^{out}/P^{in}) = 1$. This verifies the physical arguments that link the secondary effect to Poisson's ratio.

With increase in Z , the eccentricity effect increases and passes a maximum (which is discussed below), and for large values of Z all the curves merge into one. This indicates that for large Z the primary effect remains the sole contributor to the total eccentricity effect.

In Fig. 5 the curve for $\nu = 0.3$ and simple supports is redrawn, but with the computed points to

bring out the dominant dependence of the eccentricity effect on the shell geometry. Again, as is [20] and [21], the Batdorf parameter, $Z = (1 - \nu^2)^{1/2} (L/R)^2 (R/h)$, represents the shell geometry rather well. The scatter of the points about the (P^{out}/P^{in}) curve is mainly caused by the necessary periodicity of the waves in the circumferential direction, which would appear as ripples if the values of P^{out} or P^{in} were plotted versus Z . The curves in Figs. 4 and 5 smooth out the effect of these ripples on the ratio (P^{out}/P^{in}) . As Z increases further, the (P^{out}/P^{in}) curve approaches asymptotically a value larger than 1, since in the case of long shells under axial compression the buckling pattern divides the shell into "sub-cylinders" having the same critical load and hence the length ceases to affect the buckling load beyond a certain (L/R) . One may observe for example in Table 1 that for $(R/h) = 2000$ the length ceases to influence the buckling load beyond $(L/R) = 1$.

The maximum which appears in the curves of Figs. 4 and 5 represents a general characteristic behavior of stringer-stiffened cylindrical shells under axial compression that is caused by the primary effect described in Section 4. The primary effect is represented there by Eqs. (32) and (33) and depends mainly on the magnitude of the governing factors $N_x z_1$ and M_x . The larger $N_x z_1$ is compared to M_x ; the more pronounced is the difference between shells with stiffeners on the outside and those with stiffeners on the inside. One could, therefore, expect a monotonous rise of the eccentricity effect with Z , since N_x remains relatively large even for long shells, while M_x (which depends on $w_{,xx}$) decreases rapidly. However, in this discussion only the forces and moments in the axial direction have been considered, whereas actually also circumferential forces and moments contribute to the resistance against buckling. The relative contribution of N_ϕ and even more so of M_ϕ grows as Z increases. But since for a stringer stiffened shell N_ϕ and M_ϕ are practically unaffected by e_1 , the rise in (P^{out}/P^{in}) is slowed down by this "neutral" influence as Z increases, and eventually is changed to a decline.

Or, more precisely: up to $Z \approx 500$, stringers are very effective since they influence N_x and M_x , which predominate in this range of Z . On the other hand, long shells, with large Z , behave approximately as unstiffened shells, and M_ϕ , which is here unaffected by the eccentricity, overshadows the other factors. Between these two extremes there is a range of Z where axial and circumferential forces and moments make similar contributions to the stiffness of the shell. This is the range where the maximum eccentricity effect occurs.

The variation of (P^{out}/P^{in}) with Z is plotted in Fig. 5 also for clamped cylindrical shells, and clamping implies here the classical clamped boundary condition given by Eqs. (16). The behavior of the total eccentricity effect for clamped cylindrical shells is seen to be very similar to that of simply supported shells. (P^{out}/P^{in}) again has a maximum, which, however, is of slightly smaller magnitude than that for simple supports and occurs at a larger Z . The total eccentricity effect also falls off more slowly with Z for the clamped shell than for the simple supported one and outside stringers remain noticeably better than inside ones even at very high values of Z . The scatter of the points about the (P^{out}/P^{in}) curve is wider here than for simple supported shells. In clamped shells the scatter is partly caused by the necessary integer values of the number of circumferential waves, as for simple supports, and partly by the appearance of longitudinal antisymmetric buckling modes (see Table 1). The physical explanation of the eccentricity effect, discussed in Section 4, applies also to clamped shells, and indeed the main influence of the clamping of the eccentricity effect seems to be a shifting of the (P^{out}/P^{in}) curve to higher values of Z .

Fig. 6 shows the structural efficiencies of eccentrically stiffened shells. For a typical stringer geometry, the ratio of the buckling load of stiffened shells to that of equivalent unstiffened shells is plotted versus Z for outside, inside and centrally placed stringers and for simple supports and clamped ends. Equivalency here implies identical weight. The critical loads of clamped stiffened shells are actually compared with those of equivalent unstiffened shells on simple supports instead of clamped ends. However, except for very low values of Z (not represented in Fig. 6) unstiffened shells with clamped ends have practically the same buckling loads as simply supported ones, see [24], and hence the comparison is valid. Note also that the buckling loads are calculated with linear theory, and hence the values for unstiffened shells are unrealistic. Hence the curves in Fig. 6 are conservative and the actual structural efficiency of stiffened shells is higher than that shown in Fig. 6. In Figs. 11 and 12 below, the structural efficiencies of stiffened shells is reevaluated by comparison with empirical buckling loads of the unstiffened shells.

In the computations, some interesting results were obtained for M_x in shells with inside stiffeners. According to Eqs. (32) and (33), M_x^{out} and M_x^{in} are increased and decreased respectively by the influence of the membrane forces. The validity of Eqs. (32) and (33), and the physical explanation they represent,

is confirmed by the numerical results. In certain cases it was found that M_x is not only decreased for inside stringers but actually changes sign (for example, for the typical shell $(R/h) = 250$, $(L/R) = 4.0$, $(A_1/bh) = 0.5$, $(e_1/h) = 5$ and $(I_{11}/bh^3) = 5$). This means, that in certain cases, a negative moment M_x has to be applied for a positive curvature of the shell in order to reduce the positive moment contribution of the eccentrically applied membrane forces (see Fig. 2). In the mathematical formulation, Eqs. (2), this change of sign of M_x means that the bending stiffness of the shell-stiffener combination, represented here by $(1 + \eta_{01})w_{,xx}$, is overshadowed by the term $-\zeta_1 u_{,x}$ that represents the bending contribution of the membrane forces.

In Fig. 7 and Table 3, the influence of stiffener geometry parameters on the buckling load is investigated for 3 typical shells. The variation of (P^{out}/P_{UNS}) and (P^{in}/P_{UNS}) with magnitude of eccentricity, cross-sectional area and moment of inertia of stringers is plotted, where P_{UNS} is the classical buckling load of the unstiffened shell. Except for very low values of Z , the buckling load is not increased appreciably by variation of (I_{11}/bh^3) , (e_1/h) and (A_1/bh) . Indeed, in long shells with inside stringers increase of eccentricity, (e_1/h) , reduces the buckling load below that of the equivalent orthotropic cylinder, $(e_1/h) = 0$. This behavior can also be observed in Fig. 6, where the curve for $(e_1/h) = 5$ falls below that for $(e_1/h) = 0$ as Z increases beyond 300.

In Figs. 8 and 9 and Table 2, the influence of stringer cross-sectional area A_1 and magnitude of eccentricity e_1 on the eccentricity effect is investigated. The moment of inertia of the stringer about its centroid I_{11} is only a parameter of secondary importance, since it does not influence χ_1 and ζ_1 which determine the eccentricity effect. In all the curves in Figs. 8 and 9 a maximum occurs at almost the same value of Z . Even a radical change in magnitude of eccentricity from $(e_1/h) = 1$ to $(e_1/h) = 10$ causes only a slight shift in the position of the maximum from $Z = 200$ to $Z = 800$. In very heavily stiffened shells, for example, $(A_1/bh) = 3$ and $(A_1/bh) = 5$ with $(e_1/h) = 10$ in Table 5, differences in buckling load of more than 500% are obtained between outside and inside stringers. Such stringers are not realistic, but they indicate that the (P^{out}/P^{in}) ratio continues, in principle, to rise monotonically with increasing stiffener rigidity.

The torsional rigidity of the stiffener η_{t1} has been neglected in the preceding discussion. For the case of ring stiffened cylindrical shells under torsion [21], the influence of the torsional rigidity was

found to be appreciable for certain geometries. Hence the influence of η_{t1} on the buckling load is investigated here in Fig. 10 and Table 7. The range of values of $\eta_{t1} = 5$ to $\eta_{t1} = 40$ considered, is realistic and represents fairly large stringers with open and closed sections. The influence of the torsional rigidity of the stiffeners is larger for inside stringers, and is important here, in the case of axial compression, even for large Z that represent practical design dimensions. For example, for $\eta_{t1} = 10 - 20$, increases of 20–30% in buckling loads are found in Table 7, or increases of up to 25% in Table 8, where the theoretical calculations are correlated with the experimental results of [9].

The buckling loads of the stiffened and unstiffened cylindrical shells compared in the discussion were calculated by linear small deflection theory. For unstiffened cylinders under axial compression, experimental results are well known to be much below the buckling loads computed with linear theory. Closely stiffened shells, on the other hand can be adequately analysed by linear theory as is seen from the experimental confirmation given for example in [29] for ring-stiffened cylinders and [9] for stringer-stiffened shells. Hence, if one wants a clearer picture of the effectiveness of stringers as stiffeners of axially compressed cylindrical shells, one has to correct the buckling loads of the unstiffened shells, considered in Fig. 6, according to experimental results. An empirical formula for this correction is proposed in [30]. According to Fig. 3 of the same reference, the correction, Eqs. (34) below, is conservative in comparison with test results of 14 different investigators. The proposed correction factor is

$$K = (P_{oor}/P_{UNS}) = 1 - 0.901 (1 - e^{-\frac{1}{16}\sqrt{(R/h)}}) \quad (34)$$

The influence of the length of the shell on K has not been explored in great detail in [30] or earlier investigations. Preliminary experimental studies discussed in [30] indicate that the length has only a small effect on the correction factor K of Eq. (34), and length is therefore not included in the empirical correction employed here.

Fig. 11 compares the buckling load of axially compressed stringer-stiffened shells with that of equivalently thickened ones (the equivalence refers here to equal weight). The buckling loads of the equivalently thickened unstiffened shells are corrected according to Eq. (34). Hence

$$(P^{out}/\bar{P}) = (P^{out}/KP_{UNS.EQ.}) \quad (35)$$

and similarly for P^{in} . Note that \bar{P} is the critical load of an equivalently thickened shell corrected by Eq. (34). Fig. 11 is therefore a "corrected" restatement of Fig. 6 for simple supports. However, here the plot is not versus Z as in Fig. 6, but versus (R/h) , with (L/R) as an additional parameter, since the correction factor K depends on (R/h) and not on Z . The minima in (P^{out}/\bar{P}) , or (P^{in}/\bar{P}) , observed in Fig. 11 are due to different rates of decrease of K and $(P^{out}/P_{UNS.EQ.})$, with (R/h) . It is seen that outside stiffening is always better than equivalent thickening of shell irrespective of shell geometry. For inside stringers there seems to be a range of (L/R) and (R/h) for which equivalent thickening is preferable.

In Fig. 12 the influence of stiffener cross-sectional area on the "corrected" structural efficiency is studied. The cross-sectional area of the stringer is chosen as a parameter to show that increase in stiffener area may be detrimental to structural efficiency, and may mean such a weight increase that equivalent thickening is better even after the empirical correction is applied.

In Table 8 the experimental buckling loads obtained by Card [9] are compared with values calculated for classical simple supports, Eq. (6), and for classical clamped ends, Eqs. (27). Only the 4 integrally machined cylinders are compared. Theoretical values without η_{t1} and with η_{t1} are given in Table 8 and again neglect of the torsional rigidity η_{t1} is not justified here. The experimental buckling loads fall between the computed simple supports and clamped end values, slightly closer to the clamped end values. Since the test end conditions, flat ends between platens of a testing machine, are nearer to clamped ends than to simple supports, the correlation is satisfactory. For comparison, the theoretical buckling loads computed by Hedgepeth and Hall [14] for Card's test cylinders are also presented in Table 8. Hedgepeth and Hall neglect the torsional rigidity and hence their values are similar to those computed here with $\eta_{t1} = 0$. They also neglect in their theory [14] the bending and twisting stiffness of the skin, but in the case of Card's cylinders this neglect is permissible. The small differences are mainly due to slightly different interpretations of the geometries presented in [9].

A more general comparison between the theory of Hedgepeth and Hall [14] and that employed here, which was originally derived in [5], may be useful. In [14] an attempt is made to simplify the theory by neglect of "unimportant" stiffness contributions in order to facilitate deduction of general conclusions. For stringer stiffened shells the bending and twisting stiffness of the skin as well as the torsional rigidity

ty of the stringers are neglected. Hence, for simple supports, one can summarize the comparison with the present theory by the following relation

$$P = P_{HH} + [(2/n^2\beta^2)(n^2\beta^2+t^2)^2 + 2t^2\eta_{t1}] (\pi D/R) \quad (36)$$

where P is the critical axial load obtained here and P_{HH} is the critical load obtained in [14]. The importance of the torsional rigidity has already been discussed. The first term in the square brackets of Eq. (36) is important only when t is large. Hence neglect of this term is often justified, but sometimes considerable errors may result. For example, in a typical shell with $(R/h) = 500$, $(L/R) = 1.0$, $(e_1/h) = 5$, $(A_1/bh) = 1.5$ and $(I_{11}/bh^3) = 5$, the buckling load is 40% higher when the term $(2/n^2\beta^2)(n^2\beta^2+t^2)^2$ is included.

6. CONCLUSIONS

The results of the calculations for 350 typical shells under axial compression show that the behavior of the eccentricity effect depends very strongly on the geometry of the shell, while the geometry of the stiffeners only influences its magnitude. For all practical geometries outside stringers yield higher buckling loads than inside ones. The eccentricity effect had a pronounced maximum which occurs for values of Z which are common in aerospace practice. The behavior of the eccentricity effect for shells with clamped ends is very similar to that for simply supported shells. Rings are much less efficient as stiffeners. With inside rings the buckling load is reduced by the eccentricity, whereas with outside rings the axisymmetric pattern, that is not influenced by eccentricity, dominates.

ACKNOWLEDGEMENT

The authors would like to thank Mr. R. Haftka for checking of derivations, Mr. E. Glinert for assistance with the programming Mrs. J. Stern for assistance with the computations and the staff of the Technion Computing Center for their valuable help.

R E F E R E N C E S

1. Van der Neut, A., The General Instability of Stiffened Cylindrical Shells Under Axial Compression, Report S.314, National Luchtvaartlaboratorium, Amsterdam, Report and Transactions, Vol. 13, p. S.57, 1947.
2. Wilson, L.B., Deformation Under Uniform Pressure of a Circular Cylindrical Shell Supported by Equally Spaced Circular Ring Frames, Report R.337C, Naval Construction Research Establishment, St. Leonard's Hill, Dunfermline, Fife, December 1956.
3. Kendrick, S., The Buckling Under External Pressure of Circular Cylindrical Shells With Evenly Spaced Equal Strength Circular Ring Frames. Report R.211, Naval Construction Research Establishment, Dunfermline, Fife, February 1953.
4. Czerwenka, G., Untersuchungen von dünnen kurzen Zylindern die durch Ringkleinstprofile enger und mittlerer Teilung verstärkt sind und unter Manteldruck stehen, Zeitschrift für Flugwissenschaften, Vol. 10, No.6, p.163, June 1961.
5. Baruch, M. and Singer, J., Effect of Eccentricity of Stiffeners on the General Instability of Stiffened Cylindrical Shells Under Hydrostatic Pressure. Journal of Mechanical Engineering Science, Vol. 5, No. 1, p.23, March 1963.
6. Baruch, M. and Singer, J., General Instability of Stiffened Circular Conical Shells Under Hydrostatic Pressure. The Aeronautical Quarterly, Vol. 26, Part 2, p. 187, May 1965. Also Technion Research and Development Foundation, Haifa, Israel, TAE Report 28, July 1963.
7. Baruch, M., Singer, J. and Harari, O., General Instability of Conical Shells With Non-Uniformly Spaced Stiffeners Under Hydrostatic Pressure. Proceedings of the 7th Israel Annual Conference on Aviation and Astronautics, February 1965, p. 62. Also Technion Research and Development Foundation, Haifa, Israel, TAE Report 37, December 1964.
8. Houghton, D.S. and Chan, A.S.L., Design of a Pressurised Missile Body, Aircraft Engineering, Vol.

- 32, No. 381, p.320, November, 1960.
9. Card, M.F., Preliminary Results of Compression Tests on Cylinders with Eccentric Longitudinal Stiffeners, NASA TM X - 1004, September 1964.
 10. De Luzio, A.J., Stuhlman, C.E. and Almroth, B.O., Influence of Stiffeners Eccentricity and End Moment on the Stability of Cylinders in Compression, Presented at the AIAA 6th Structures and Materials Conference, Palm Springs, 5-7 April, 1965.
 11. Garkisch, H.D., Geier, B. and Seggelke, P. Beulversuche an langversteiften Zylinderschalen (to be published as DLR - FB).
 12. Van der Neut, A., General Instability of Orthogonally Stiffened Cylindrical Shells, Collected Papers on Instability of Shell Structures - 1962, NASA TN D-1510, p.309, December 1962.
 13. Hedgepeth, J.M., Design of Stiffened Cylinders in Axial Compression, Collected Papers on Instability of Shell Structures - 1962, NASA TN D-1510, p.77, December 1962.
 14. Hedgepeth, J.M. and Hall, D.B., Stability of Stiffened Cylinders, Presented at the AIAA 2nd Aerospace Sciences Meeting, New York, 25-27 January, 1965.
 15. McElman, J.A., Mikulas, M.M. and Stein, M., Static and Dynamic Effects of Eccentric Stiffening of Plates and Cylindrical Shells. Presented at the 2nd AIAA Annual Meeting and Technical Display, San Francisco 26-29 July 1965.
 16. Block, D.L., Card, M.F. and Mikulas, M.M., Buckling of Eccentrically Stiffened Orthotropic Cylinders, NASA TN D-2960, August 1965.
 17. Geier, B. and Seggelke, P. - Das Beulverhalten versteifter Zylinderschalen, Teil 2, Beullasten bei axial-symmetrischer Belastung, (to be published in Zeitschrift fur Flugwissenschaften).
 18. Crawford, R.F., Effects of Asymmetric Stiffening on Buckling of Shells, Presented at the 2nd AIAA Annual Meeting and Technical Display, San Francisco 26-29 July 1965.

19. Thielemann, W. and Esslinger, M., Über den Einfluss der Exzentrizität von Längssteifen auf die axiale Beullast dünnwandiger Kreiszyinderschalen, (to be published as a DLR – FB).
20. Singer, J., Baruch, M. and Harari, O., Further Remarks on the Effects of Eccentricity of Stiffeners on the General Instability of Stiffened Cylindrical Shells, Technion Research and Development Foundation, Haifa, Israel, TAE Report 42, August 1965.
21. Baruch, M., Singer, J. and Weller, T., Effect of Eccentricity of Stiffeners on the General Instability of Stiffened Cylindrical Shells Under Torsion. Technion Research and Development Foundation, Haifa, Israel, TAE Report 43, August 1965.
22. Batdorf, S.B., Simplified Method of Elastic Stability Analysis for Thin Cylindrical Shells, NACA Report 874, 1947.
23. Hoff, Nicholas J., Low Buckling Stresses of Axially Compressed Circular Cylindrical Shells, SUDAER No. 192, Stanford University, July 1964.
24. Hoff, N.J. and Soong, T.C., Buckling of Circular Cylindrical Shells in Axial Compression, SUDAER No. 204, Stanford University, July 1964.
25. Almroth, B.O., Influence of Edge Conditions on the Stability of Axially Compressed Cylindrical Shells, NASA CR 161, February 1965.
26. Thielemann, W. and Esslinger, M., Einfluss der Randbedingungen auf die Beullast von Kreiszyinderschalen, Der Stahlbau, Vol. 33, No. 12; p.3, December 1964.
27. Timoshenko, S.P. and Gere, J.M., Theory of Elastic Stability, McGraw-Hill Book Co., New York, 1961, Chapter 11.
28. Thielemann, W.F., New Developments in the Nonlinear Theories of the Buckling of Thin Cylindrical Shells, Aeronautics and Astronautics, Proc. of Durand Centennial Conference, Stanford 1959, Pergamon Press, Oxford, 1960, p. 76.

29. Gerard, G., Elastic and Plastic Stability of Orthotropic Cylinders, Collected Papers on Instability of Shell Structures - 1962, NASA TN D-1510, P.277, December 1962.
30. Weingarten, V.I., Morgan, E.J. and Seide, Paul, Elastic Stability of Thin-Walled Cylindrical and Conical Shells Under Axial Compression, AIAA Journal, Vol. 3, No. 3, p.500, March 1965.

TABLE 1.

AXIAL LOAD PARAMETER λ FOR STRINGER STIFFENED CYLINDERS

EFFECT OF SHELL GEOMETRY for CLAMPED & SIMPLY SUPPORTED BOUNDARY CONDITIONS

$A_1/bh = 0.5$ $I_{11}/bh^3 = 5$ $e_1/b = \pm 5$ $\nu = 0.3$

L/R	R/h	Z	SIMPLY SUPPORTED												CLAMPED									
			$e_1 > 0$ inside			$e_1 = 0$			$e_1 < 0$ outside			λ^+/λ_{UNS}	λ^0/λ_{UNS}	λ^-/λ_{UNS}	λ^-/λ^+	$e_1 > 0$ inside		$e_1 < 0$ outside		λ^+/λ_{UNS}	λ^-/λ_{UNS}	λ^-/λ^+		
			λ^+	t	n	λ^0	t	n	λ^-	t	n					λ^+	t	λ^-	t					
0.25	50	2.981	46640	8	1				46360	3	1	70.50		70.08	0.994									
0.35	50	5.843	23890	7					23650	0**		28.48		28.19	0.990									
0.5	50	11.92	11800	6	1	4991	6	1	12110	0		17.84	7.545	18.30	1.026	46700	8	46360	3	70.66	70.08	0.992		
	100	23.85	12050	8		5714	9	1	14830	5		9.095	4.311	11.19	1.231	47000	9	46380	1	35.46	34.99	0.987		
	250	59.62	12980	11					20050	12		3.868		5.973	1.544									
	500	119.2	15030	14					26440	16		2.275		4.000	1.758	50170	15	64770	13	7.591	9.800	1.291		
	1000	238.5	20000	17					37640	19		1.512		2.846	1.882	55990	19	86160	20	4.234	6.315	1.539		
	2000	477.0	31590	21					58020	24		1.195		2.195	1.837	70740	24	12270	27	2.676	4.641	1.734		
1.0	50	47.70	3156	5	1	1814	6	1	4659	5		4.771	2.742	7.042	1.476	11930	6	12130	1	18.03	18.33	1.017		
	100	95.39	3551	6		2561	7	1	6016	7		2.679	1.933	4.540	1.695	12310	7	14890	4	9.285	11.23	1.210		
	250	238.5	5045	9		4914	9	1	9411	10		1.526	1.486	2.846	1.865	14030	10	21540	10	4.243	6.315	1.535		
	500	477.0	7933	11		8865	11	1	14500	12		1.200	1.341	2.195	1.828	17690	12	30720	13	2.676	4.649	1.737		
	1000	953.9	14300	13		16860	14	1	24030	14		1.081	1.275	1.817	1.680	26480	15	47260	17	2.002	3.575	1.785		
	2000	1908	28080	16					42280	17		1.062		1.599	1.506	45200*	23	78200	21	1.710	2.960	1.731		
	5000	4770	70650	28	2				94870	21		1.069		1.435	1.343	90000*	31	156000*	33	1.362	2.562	1.734		
	50000	47700	701900	80	5				847600	38		1.062		1.282	1.207									
1.5	50	107.3	1648	4	1				2805	5		2.494		4.239	1.701									
	100	214.6	2160	6					3961	6		1.630		2.988	1.834									
	250	536.6	3908	7					6985	8		1.182		2.112	1.787									
2.0	100	381.6	1673	5	1				3193	6		1.262		2.409	1.909									
	250	953.9	3693	7					6008	7		1.117		1.817	1.627									
	500	1908	7020	8		8219	8	1	10700	8		1.062	1.244	1.620	1.525									
	2000	7632	28080	16	2	32410	12	1	36590	12		1.062	1.226	1.384	1.303									
4.0	50	763.2	731.7	3	1				1326	3		1.106		2.005	1.812	1507	4	2551	4	2.277	3.856	1.693		
	100	1526	1454	4	1				2191	4		1.100		1.657	1.507	2513	5	4140	5	1.901	3.132	1.647		
	250	3816	3608	5	1				4843	5		1.091		1.465	1.342	4670*	7	8280*	8	1.413	2.505	1.773		
	500	7632	7020	8	2				9148	6		1.062		1.384	1.303	8434	10	14230*	9	1.276	2.153	1.687		
	1000	15260	14200	12	3				17610	7		1.074		1.332	1.241									
	2000	30530	28080	16	4	32410	12	2	34930	8		1.062	1.226	1.321	1.244	29914	18	45920	16	1.131	1.737	1.535		
6.0	250	8585	3670	4	1				4550	4		1.110		1.377	1.240									
	1000	34340	14050	11	4				17270	6		1.063		1.307	1.229									
10	500	47700	7020	8	5				8713	4	1	1.062		1.318	1.241									
	20	500	190800	7020	8	10			8713	4	2	1.062		1.318	1.241									

** t = 0 means Axisymmetric Buckling

* cases where shell buckles in a longitudinal antisymmetric pattern if not otherwise mentioned this pattern is symmetric

TABLE 2.

AXIAL LOAD PARAMETER λ FOR STRINGER STIFFENED CYLINDERS

EFFECT of SHELL GEOMETRY

L/R	R/h	Z	$A_1/bh=0.5 \quad I_{11}/bh^3=5 \quad e_1/h=\pm 2$					$A_1/bh=0.5 \quad I_{11}/bh^3=5 \quad e_1/h=\pm 10$					$A_1/bh=0.5 \quad I_{11}/bh^3=15 \quad e_1/h=\pm 5$					$A_1/bh=1.5 \quad I_{11}/bh^3=5 \quad e_1/h=\pm 5$				
			inside (+)		outside (-)		λ^-/λ^+	inside (+)		outside (-)		λ^-/λ^+	inside (+)		outside (-)		λ^-/λ^+	inside (+)		outside (-)		λ^-/λ^+
			λ^+	t	λ^-	t		λ^+	t	λ^-	t		λ^+	t	λ^-	t		λ^+	t	λ^-	t	
0.5	250	59.62						33810	9	49160	10	1.454	21610	11	28670	12	1.327	18110	9	33470	9	1.848
	500	119.2						34870	12	59540	16	1.708	23660	14	35060	16	1.482	19350	12	47010	15	2.430
1.0	50	47.70	1866	5	2434	6	1.304	8413	4	11420	3	1.357	5312	5	6814	5	1.283	4492	4	7376	3	1.642
	100	95.39	2443	7	3402	7	1.393	8653	5	13980	7	1.616	5706	6	8172	7	1.432	4738	6	10580	7	2.234
	250	238.5	4395	9	6196	9	1.410	9479	8	18640	10	1.967	7201	9	11570	10	1.606	5716	8	16590	10	2.902
	500	477.0	7901	11	10620	11	1.344	11460	10	24960	12	2.178	10090	11	16660	12	1.651	8222	10	24690	13	3.003
	1000	953.9	15320	13	19120	14	1.248	16610	12	36280	14	2.184	16460	13	26190	14	1.591	14310	13	38880	15	2.717
2.0	100	381.6						2713	5	5659	6	2.086	2211	5	3732	6	1.688	1789	5	5387	6	3.011
	150	572.4						3139	5	6886	6	2.194	2878	6	4661	6	1.620	2421	6	6966	7	2.878
	1000	3816	15320*	13	17340	10	1.132	13710	9	23800	10	1.736	14970	10	19910	10	1.330	14310*	13	28630	11	2.001
3.0	100	858.5						1711	4	3824	5	2.235	1713	4	2798	5	1.633	1476	4	4017	5	2.722
	150	1288						2390	5	4862	5	2.034	2395	5	3630	5	1.516	2159	5	5526	5	2.560
	1000	8585	15190*	11	16900	8	1.113	13800	8	20840	8	1.511	14920	8	18440	8	1.236	14310**	13	25800	9	1.803

for most cases $n = 1$ (one longitudinal wave), except those marked by

$\left\{ \begin{array}{l} * \text{ for which } n = 2 \\ ** \text{ for which } n = 3 \end{array} \right.$

TABLE 3.

AXIAL LOAD PARAMETER λ FOR STRINGER - STIFFENED CYLINDERS

EFFECT of STIFFENER GEOMETRY

STIFFENER GEOMETRY			L/R = 0.5 R/h = 100 Z = 23.85						L/R = 2.0 R/h = 500 Z = 1900						L/R = 4.0 R/h = 2000 Z = 30500								
A_1/bh	I_{11}/bh^3	$ e_1/h $	inside (+)		outside (-)		λ^+/λ_{UNS}	λ^-/λ_{UNS}	λ^-/λ^+	inside (+)		outside (-)		λ^+/λ_{UNS}	λ^-/λ_{UNS}	λ^-/λ^+	inside (+)		outside (-)		λ^+/λ_{UNS}	λ^-/λ_{UNS}	λ^-/λ^+
			λ^+	t	λ^-	t				λ^+	t	λ^-	t				λ^+	t	λ^-	t			
0.1	5	5	7293	8	8064	9	5.503	6.085	1.106	6925	8	7689	8	1.048	1.163	1.110	27390	11	28210	8	1.036	1.067	1.030
0.3			9963	8	12020	8	7.518	9.072	1.207	6973	8	9224	8	1.055	1.396	1.323	27900	16	31590	8	1.055	1.195	1.132
0.5			12050	8	14830	5	9.095	11.19	1.231	7020	8	10700	8	1.062	1.620	1.525	28080	16	34930	8	1.062	1.321	1.244
0.7			13650	7	16530	2	10.30	12.48	1.211								28260	16	37720	9	1.069	1.427	1.335
1.0			15490	7	18040	0	11.69	13.61	1.164	7130	8	13650	9	1.079	2.066	1.915	28410	18	41070	9	1.075	1.553	1.445
1.5			17660	6	19750	0	13.32	14.91	1.119	7230	8	16260	9	1.094	2.460	2.249	28450	18	46570	9	1.076	1.761	1.637
0.5	1	5	8605	8	11380	5	6.493	8.990	1.323	6804	8	10490	8	1.029	1.587	1.542	26930	19	34880	8	1.019	1.319	1.295
	3		10330	8	13110	5	7.794	9.891	1.269	6912	8	10600	8	1.046	1.603	1.533	27650	16	34900	8	1.046	1.320	1.262
	10		16360	8	19140	5	12.35	14.45	1.170	7289	8	10970	8	1.103	1.660	1.505	29010	14	35000	8	1.097	1.324	1.206
	15		20680	8	23460	5	15.60	17.70	1.134	7559	8	11240	8	1.144	1.701	1.487	29610	14	35060	8	1.120	1.326	1.184
	20		24990	8	27770	5	18.85	20.95	1.111								30220	14	35130	8	1.143	1.329	1.163
0.5	5	0	5714	9			4.311		1	8219	8			1.244		1	32410	12			1.226		1
		1	5729	9	6344	9	4.323	4.787	1.107	7876	8	8613	8	1.192	1.303	1.094	31480	14	33140	12	1.191	1.254	1.053
		3	7641	8	9477	8	5.766	7.151	1.240	7345	8	9556	8	1.111	1.446	1.301	29350	18	34010	8	1.110	1.286	1.159
		7	18810	7	21460	0	14.19	16.19	1.141								27570	14	35900	8	1.043	1.358	1.302
		10	33400	6	35220	0	25.20	26.98	1.054	7107	8	14300	9	1.075	2.164	2.012	27190	14	37460	8	1.028	1.417	1.378

TABLE 4. INFLUENCE OF POISSON'S RATIO ON ECCENTRICITY EFFECT

$A_1/bh=0.5 \quad I_{11}/bh^3=5 \quad e_1/h=\pm 5$

L/R	0.35	0.5		1.0					
R/h	50	50	100	50	100	250	500	2000	5000
Z	5.843	11.92	23.85	47.70	95.39	238.5	477	1908	4770
λ^+ (inside +)	26070	12860	13070	3421	3811	5348	8350	28140	74300
$\nu=0 \quad \lambda^-$ (outside -)	26690	14230	17480	5299	6737	10310	15690	44990	100600
λ^-/λ^+	1.024	1.107	1.337	1.549	1.768	1.928	1.879	1.599	1.354
$\nu=0.3$									
λ^+	23890	11800	12050	3156	3551	5045	7933	28080	70650
λ^-	23650	12130	14830	4659	6016	9411	14500	42280	94870
λ^-/λ^+	0.990	1.026	1.231	1.476	1.695	1.865	1.828	1.506	1.343
$\nu=0.5$									
λ^+	19860	9830	10070	2660	3027	4425	7103	25640	63890
λ^-	19540	9699	11660	3759	4967	8027	12600	37610	85210
λ^-/λ^+	0.984	0.987	1.159	1.413	1.641	1.814	1.774	1.467	1.334

TABLE 5.

ECCENTRICITY EFFECT FOR CYLINDRICAL SHELLS WITH HEAVY STRINGERS

L/R	R/h	A_1/bh	I_{11}/bh^3	$ e_1/h $	inside (+)		outside (-)		λ^-/λ^+
					λ^+	t	λ^-	t	
1.0	250	1.5	5	7	8432	7	23380	10	2.891
	500				10150	10	33900	13	3.340
	1000				15180	13	50060	15	3.299
1.0	250	1.5	5	10	14780	7	39700	10	2.686
	500				15730	9	51720	13	3.288
	1000				19240	12	70690	16	3.674
2.0	500	1.5	5	10	7471	8	25890	9	3.465
		3.0			7597	7	39650	10	5.220
		5.0			13970	10	81770	12	5.852

TABLE 6. RING STIFFENED CYLINDERS UNDER AXIAL COMPRESSION

AXISYMMETRIC AND ASYMMETRIC

$L/R=0.5$ $\nu=0.3$

R/h	A_2/ah	I_{22}/ah^3	e_2/h	inside rings (+)			outside rings (-)			λ^+/λ_{UNS}	λ^-/λ_{UNS}
				λ^+	t	n	λ^-	t	n		
50	0.5	5	5	718.4	3	2	809.4	0*	2	1.086	1.223
100				1420	4	3	1619		3	1.072	1.222
250				3578	6	5	4048		5	1.066	1.206
500				7063	8	6	8094		6	1.062	1.211
1000				14050	11	9	16190		9	1.062	1.224
2000				28080	16	13	32380		13	1.062	1.225
250	0.5	2	0	4016	5	5	**			1.196	
				4033	3	5				1.201	
				4044	2	5				1.205	
				4046	1	5				1.205	
				4048	0	5				1.206	
250	0.5	5	0.5	3994	4	5	4048	0	5	1.190	1.206
				3854	7	5	4048		5	1.148	1.206
				4030	2	5	4048		5	1.200	1.206

* t=0 means axisymmetric buckling

** results for outside and inside rings are the same because $e_2=0$

TABLE 7.

INFLUENCE OF TORSIONAL RIGIDITY OF STRINGER (η_{t1}) ON BUCKLING LOAD

$$A_1/bh=0.5 \quad I_{11}/bh^3=5 \quad e_1/h=5^\circ \quad \nu=0.3$$

L/R	R/h	Z	λ							** $\lambda_{\eta_{t1}=5}/\lambda_{\eta_{t1}=0}$	$\lambda_{\eta_{t1}=10}/\lambda_{\eta_{t1}=0}$	$\lambda_{\eta_{t1}=20}/\lambda_{\eta_{t1}=0}$		$\lambda_{\eta_{t1}=40}/\lambda_{\eta_{t1}=0}$
			$\eta_{t1}=0$		$\eta_{t1}=5$	$\eta_{t1}=10$	$\eta_{t1}=20$		$\eta_{t1}=40$			inside (+)	outside (-)	
			inside (+)	outside (-)	inside (+)	inside (+)	inside (+)	outside (-)	inside (+)					
0.5	250	59.62	12980	20050	14020	15020	16680	24370	19500	1.080	1.157	1.285	1.216	1.502
	2000	477	31590	58020	36000	40330	48330	78270	62980	1.140	1.277	1.530	1.349	1.994
1.0	50	47.7	3156	4659	3406	3611	3931	5460	4571	1.079	1.144	1.245	1.172	1.448
	250	238.5	5045	9411	5744	6384	7664	12790	9842	1.133	1.265	1.519	1.359	1.950
	2000	1908	28080	42280	30640	33200	37840	53060	46840	1.091	1.182	1.348	1.255	1.668
	5000	4770	70650	94870	76060	80060	88060	112500	103700	1.077	1.133	1.246	1.186	1.468
4.0	250	3816	3608	4843	3858	4108	4608	5843	5608	1.069	1.139	1.277	1.206	1.554

* inside stringers are considered except for $\eta_{t1}=20$ where both inside and outside configurations were checked

** $\lambda_{\eta_{t1}=a}$ means axial load parameter computed with $\eta_{t1}=a$

TABLE 8.

COMPARISON of THEORETICAL and CARD'S EXPERIMENTAL RESULTS

No	SHELL GEOMETRY		STRINGER GEOMETRY				P (kips)		P (kips) TEST Ref [9]	P (kips) obtained by [14]	
	L/R	R/h	A_1/bh	I_{11}/bh^3	e_1/h	η_{t1}	simply supp.	clamped.		simply supp.	clamped ends
1	3.98	338	1.03	9.79	-5.83	0	62.57 (6)	113.8 (7)	112.6 (6)	61.93 (6)	114.5 (7)
						17	71.61 (6)	128.0 (7)			
2	3.98	345	1.06	10.5	5.96	0	35.22 (7)	47.96 (8)	48.0 (6)	34.98 (7)	47.76 (8)
						18.2	43.15 (5)	62.82 (7)			
3	2.49	347	1.07	10.8	-6	0	71.0 (7)	142.4 (9)	127.2 (7)	70.8 (7)	143.0 (9)
						18.6	83.35 (7)	163.8 (8)			
4	2.49	341	1.05	10.1	5.89	0	36.64 (7)	63.85 (8)	61.6 (6)	35.4 (7)	61.98 (8)
						17.6	45.93 (6)	77.81 (7)			

* the number in brackets is equal to the number of circumferential waves

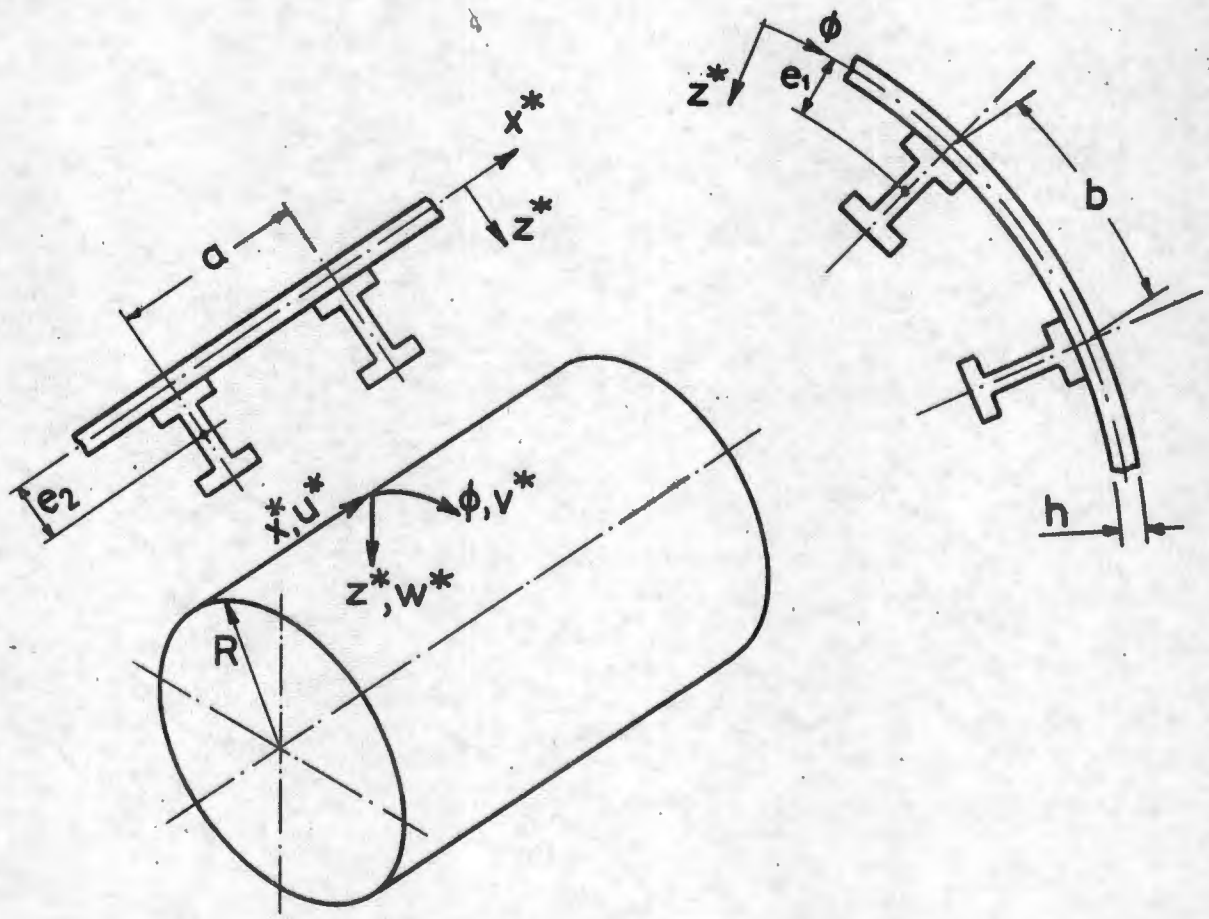
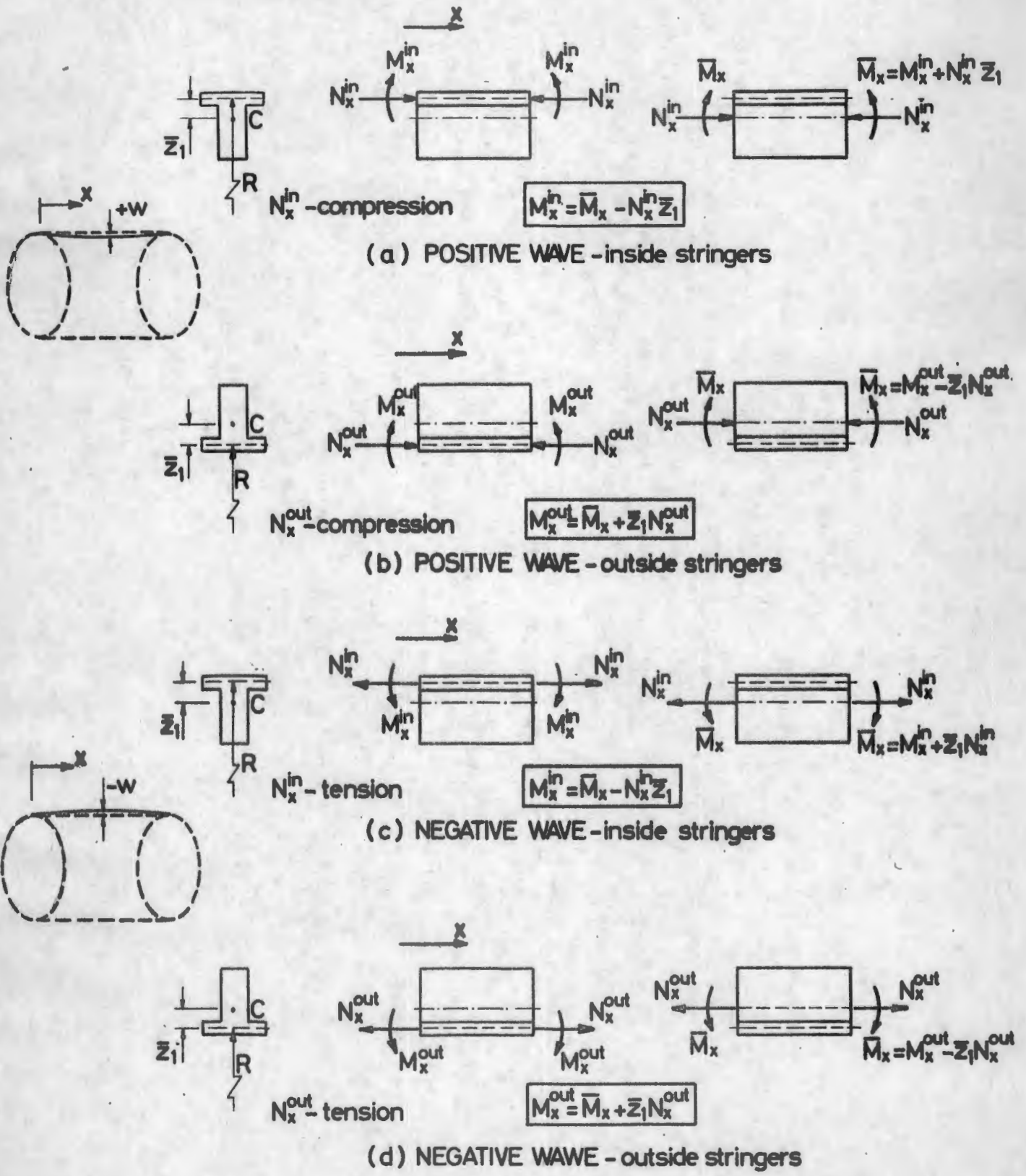


FIG. 1 NOTATION



N_x^{in} - compression

$$M_x^{in} = \bar{M}_x - N_x^{in} z_1$$

N_x^{out} - compression

$$M_x^{out} = \bar{M}_x + z_1 N_x^{out}$$

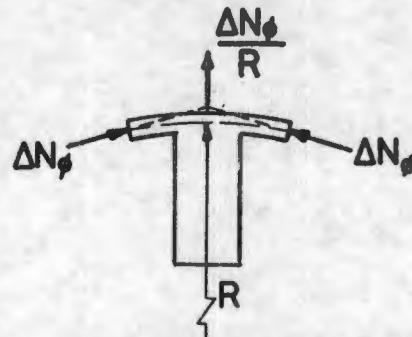
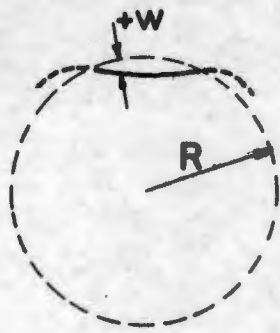
N_x^{in} - tension

$$M_x^{in} = \bar{M}_x - N_x^{in} z_1$$

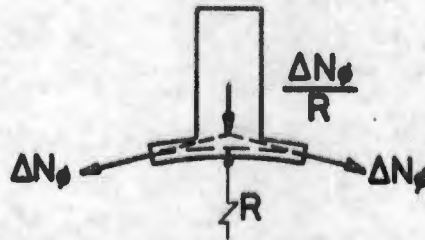
N_x^{out} - tension

$$M_x^{out} = \bar{M}_x + z_1 N_x^{out}$$

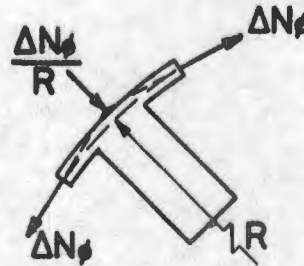
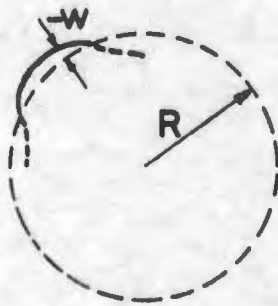
FIG. 2



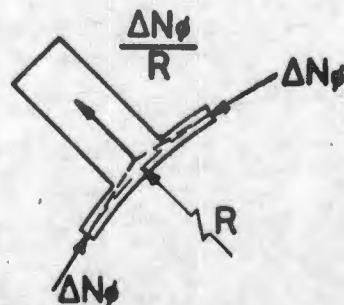
(a) POSITIVE WAVE - inside stringers



(b) POSITIVE WAVE - outside stringers



(c) NEGATIVE WAVE - inside stringers



(d) NEGATIVE WAVE - outside stringers

FIG. 3

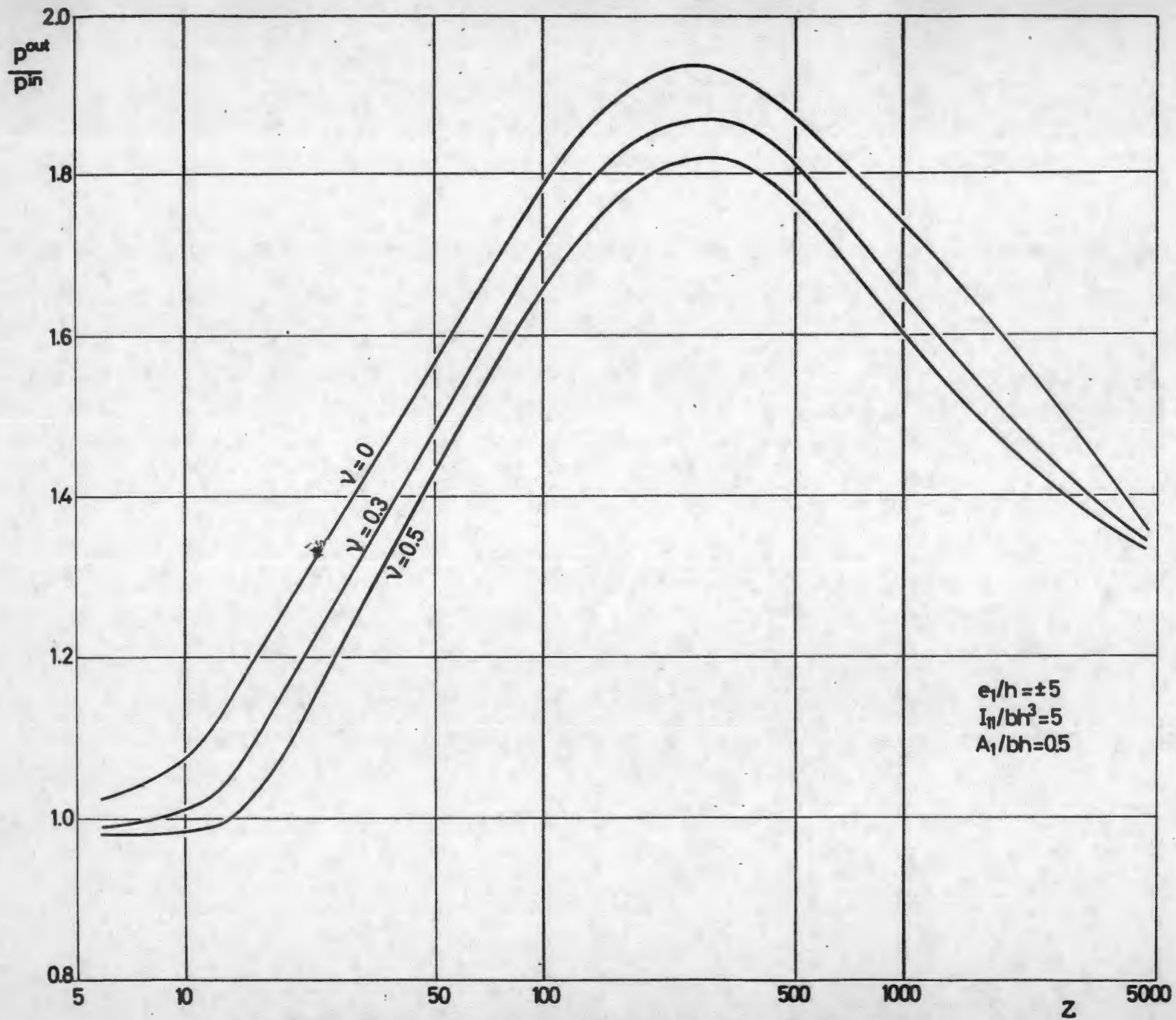


FIG.4 INFLUENCE OF POISSON'S RATIO ON THE ECCENTRICITY EFFECT

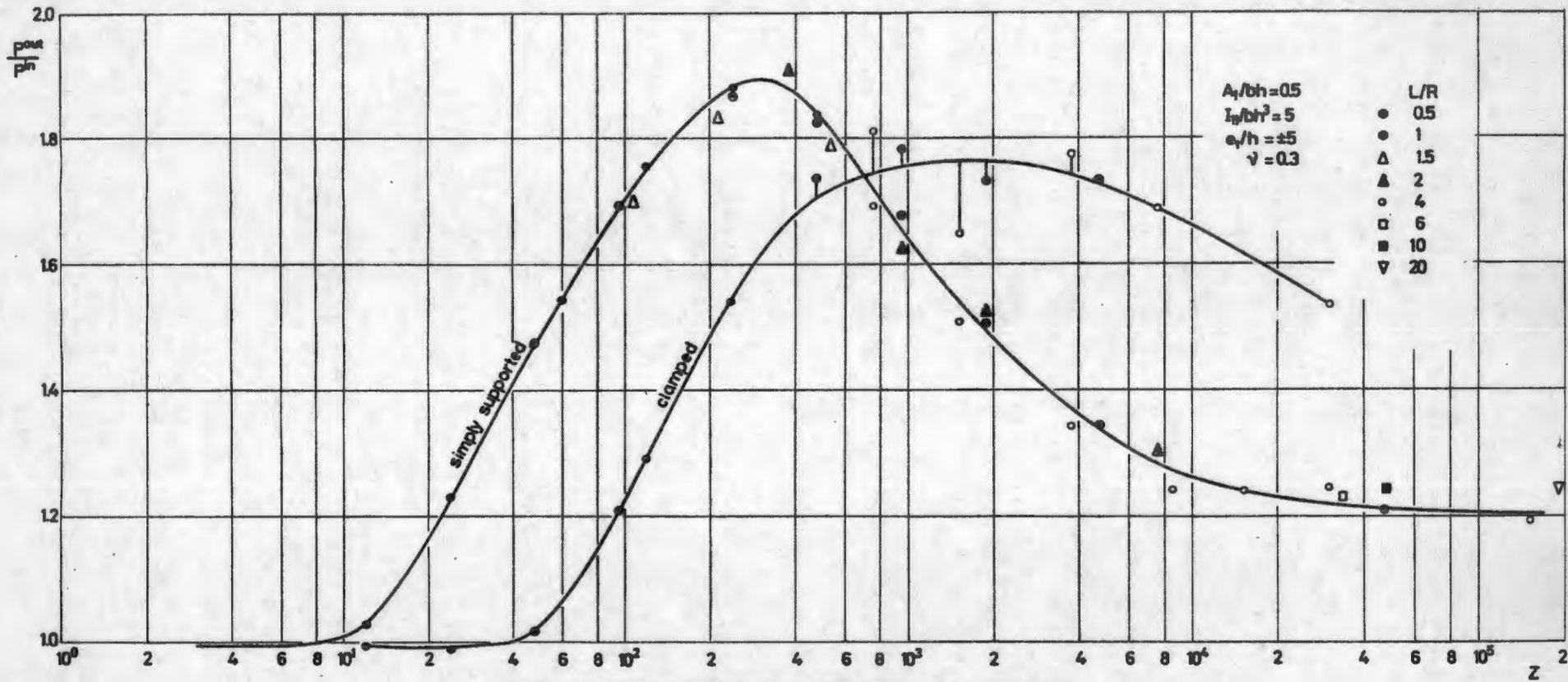


FIG.5 VARIATION OF ECCENTRICITY EFFECT WITH SHELL GEOMETRY AND BOUNDARY CONDITIONS

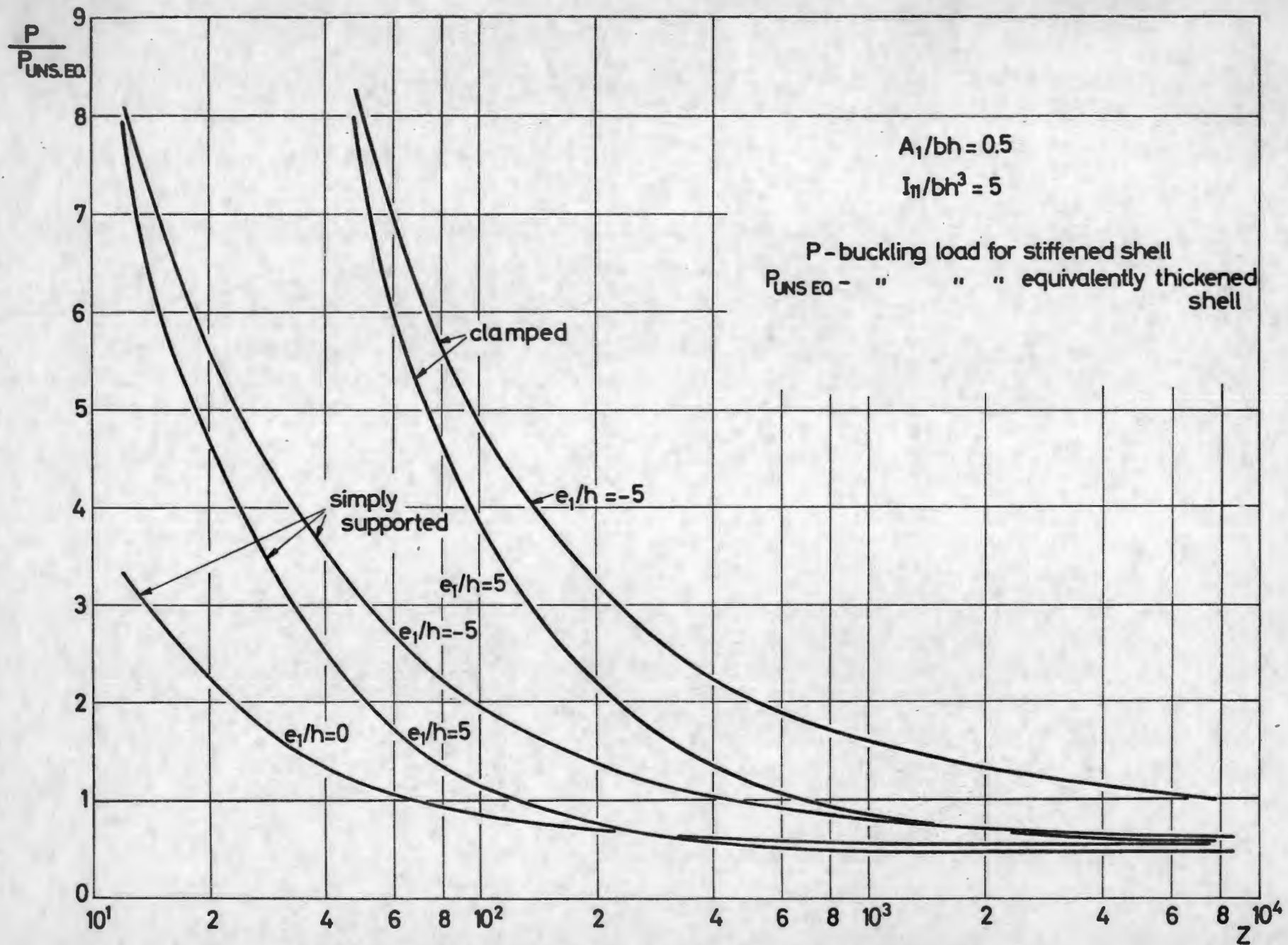


FIG. 6 EFFECT OF END CONDITIONS ON THE STRUCTURAL EFFICIENCY OF ECCENTRICALLY STIFFENED SHELLS

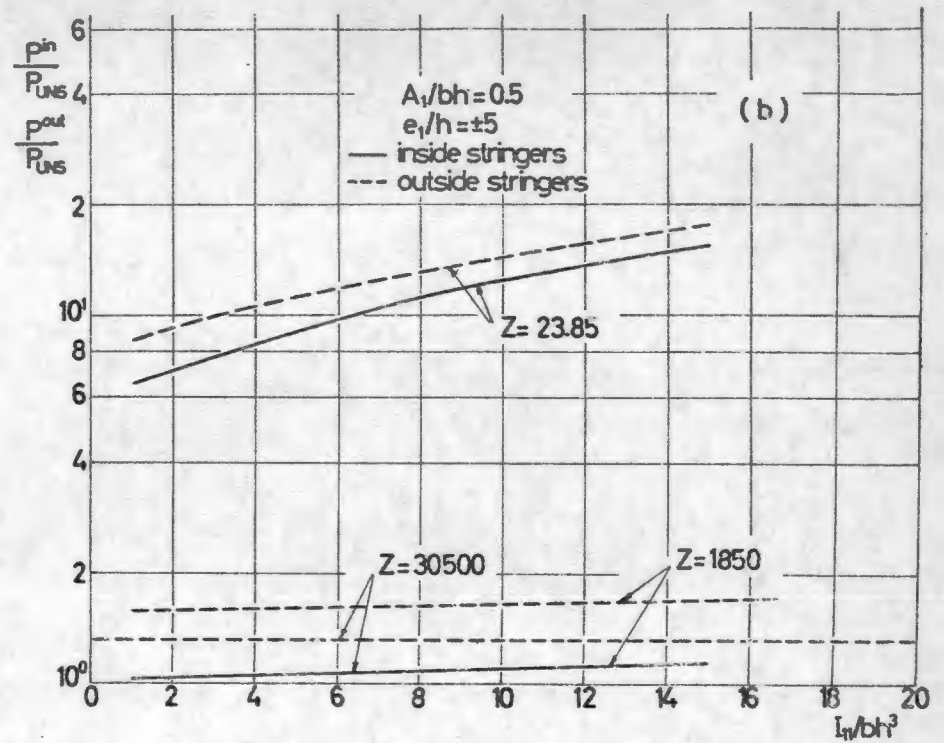
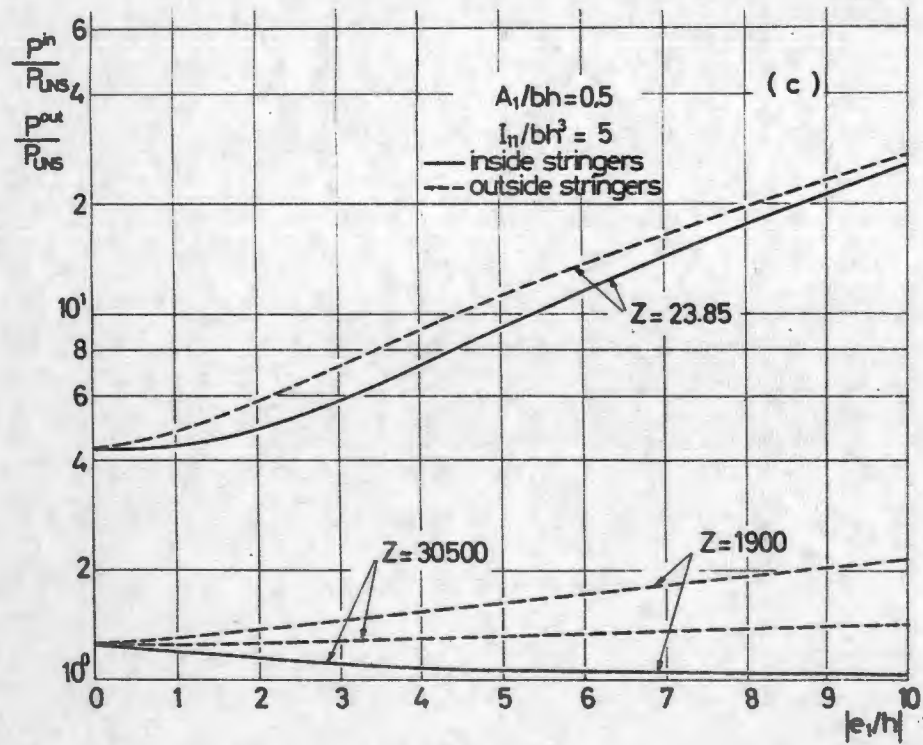
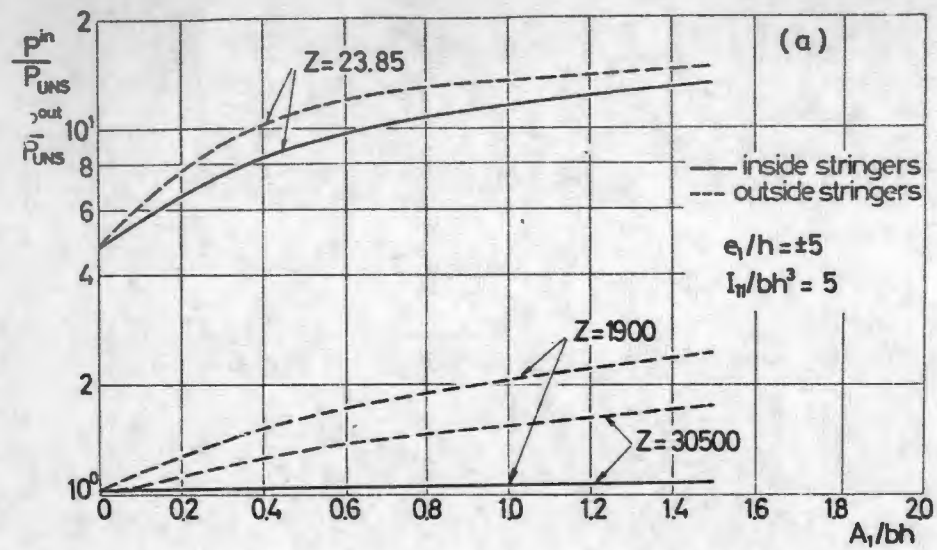


FIG. 7 EFFECT OF STIFFENER GEOMETRY ON STIFFENING OF SHELL



FIG. 8 INFLUENCE OF (A_1/bh) ON ECCENTRICITY EFFECT

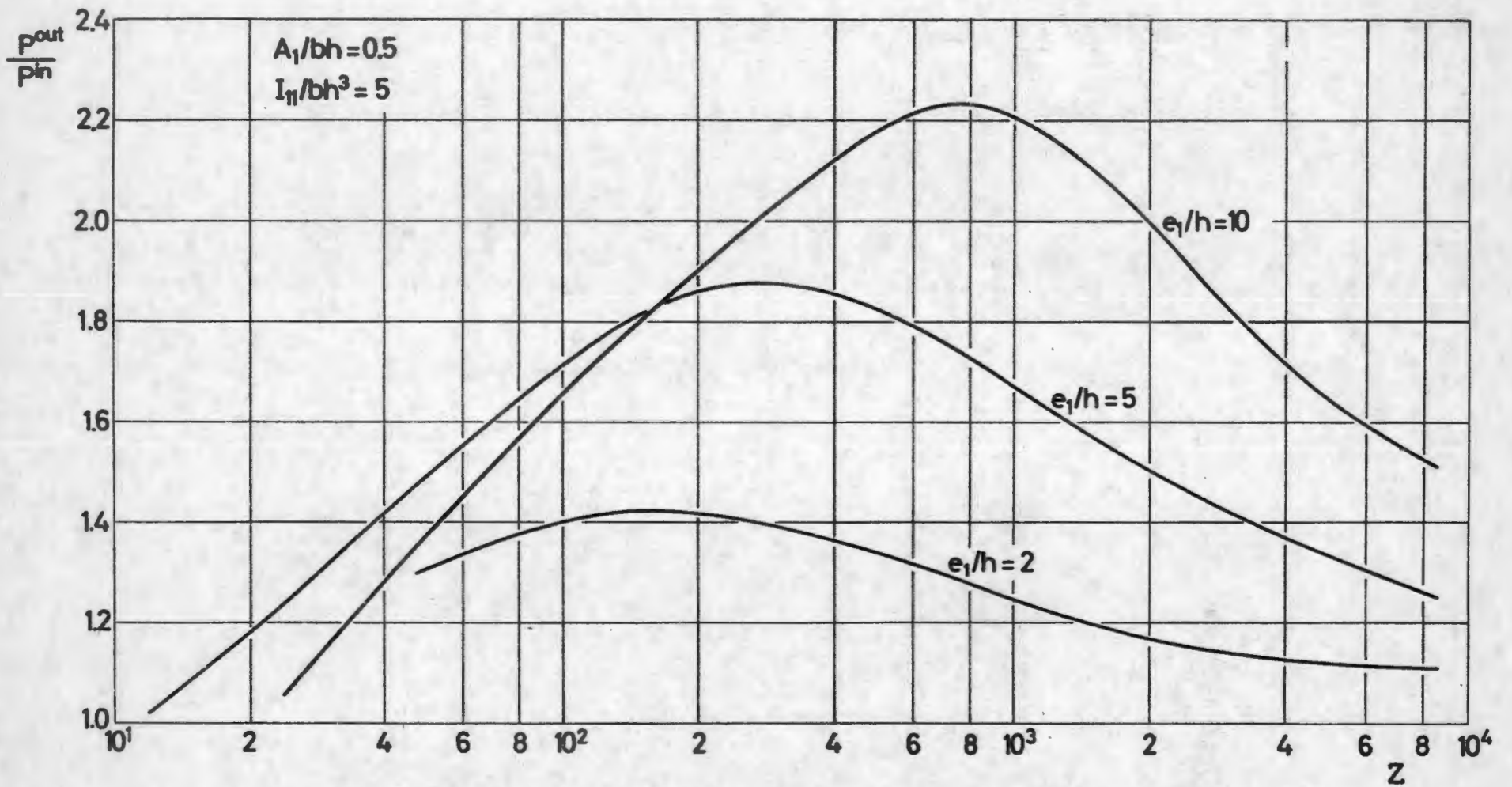


FIG. 9 INFLUENCE OF MAGNITUDE OF $|e_1/h|$ ON ECCENTRICITY EFFECT

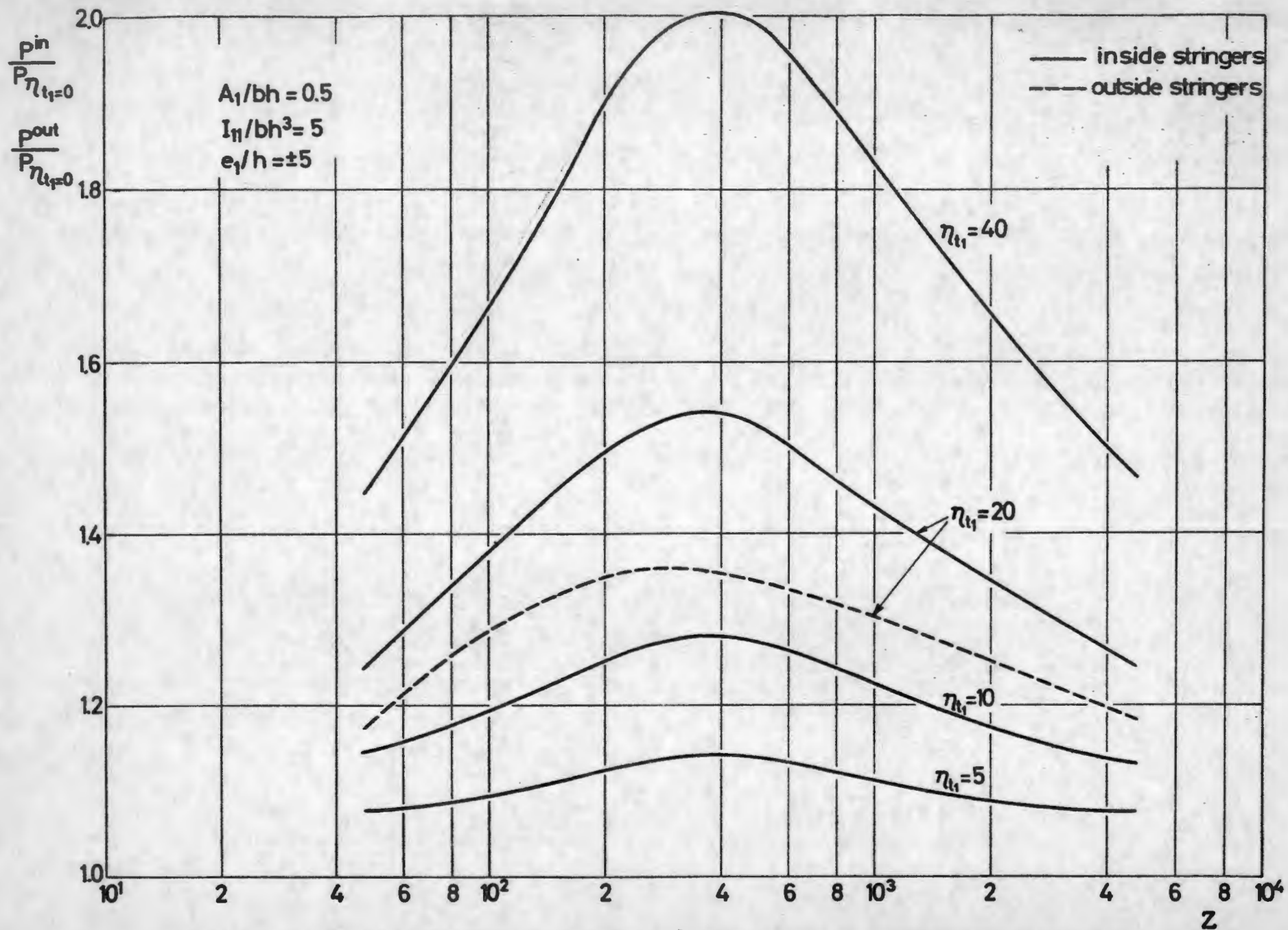


FIG. 10 INFLUENCE OF TORSIONAL RIGIDITY OF STRINGERS ON STIFFENING OF SHELLS

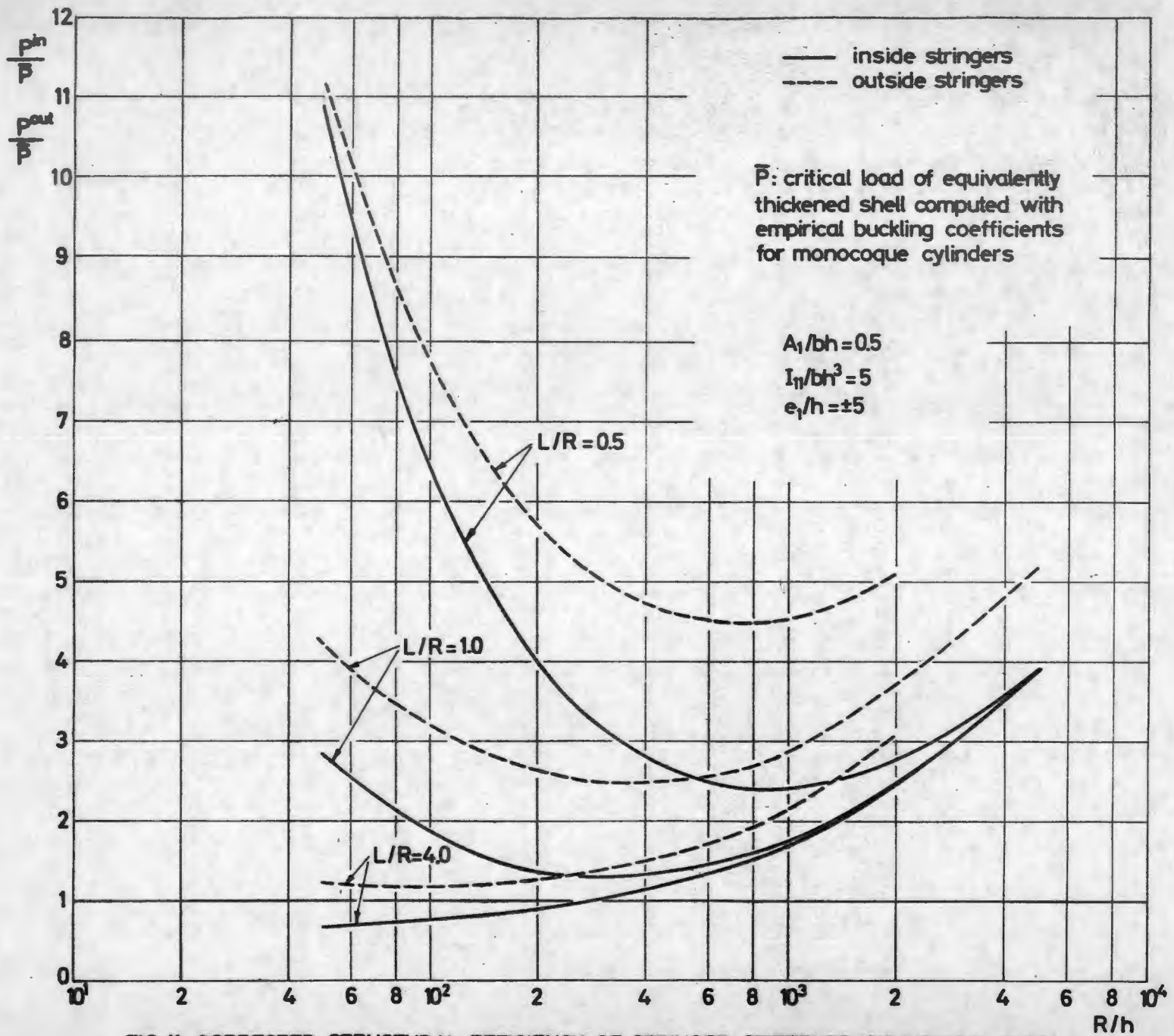


FIG. 11 CORRECTED STRUCTURAL EFFICIENCY OF STRINGER STIFFENED CYLINDRICAL SHELL WITH SIMPLE SUPPORTS

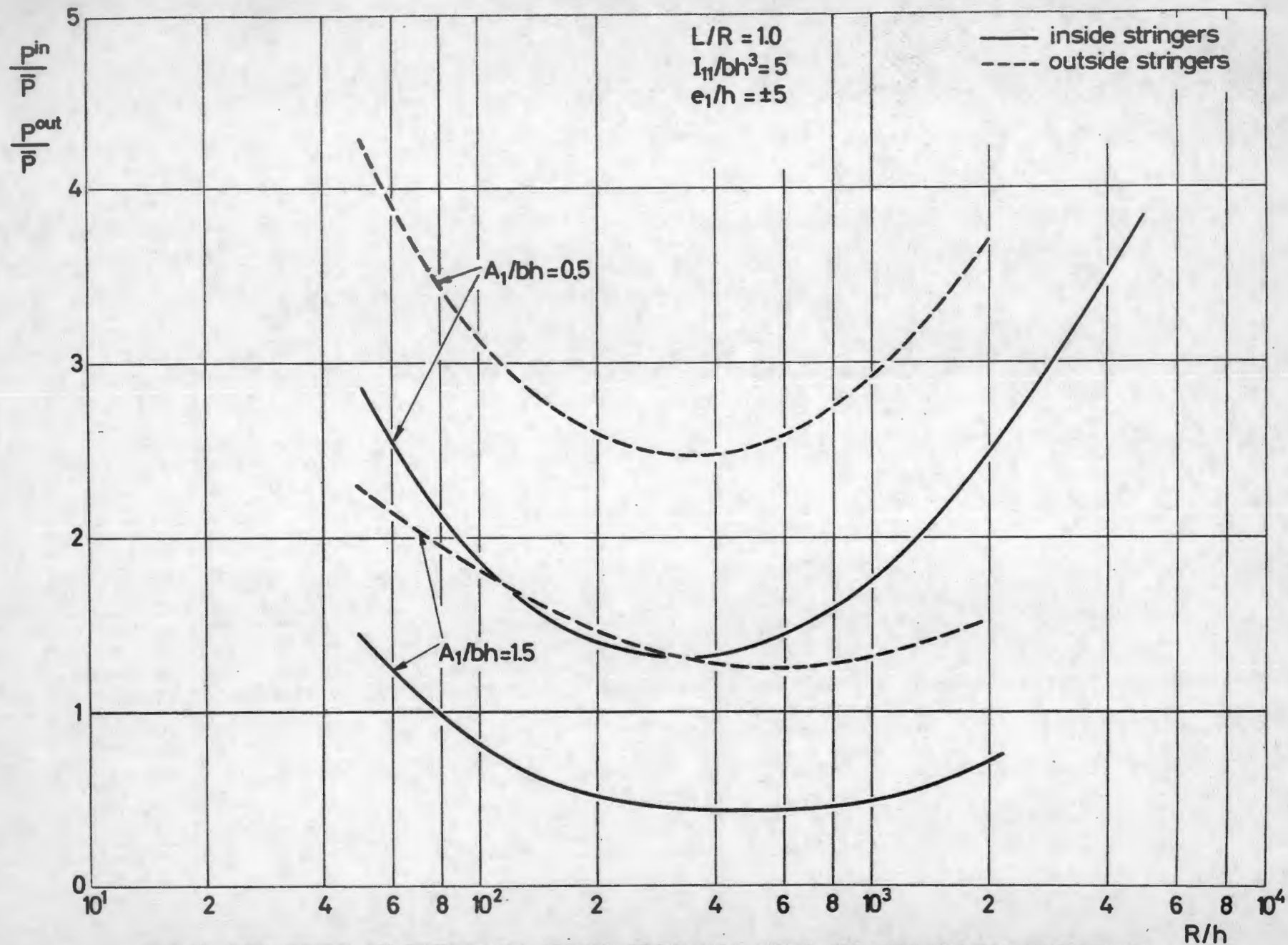


FIG. 12 INFLUENCE OF STIFFENER CROSS-SECTIONAL AREA ON STRUCTURAL EFFICIENCY OF SIMPLY SUPPORTED SHELL